as effector cells. As shown in Fig. 5 (B), the percent specific lysis obtained by our assay was in close agreement with experimental data obtained from a ^{51}Cr-release assay.

Furthermore, we examined the stability of prepared samples. After cells were resuspended with PFA-PBS, acquisition was done just after preparation and also two and three days after preparation. As shown in Table 1, almost the same percent lysis was obtained at these three acquisition times. These results indicate that we could stock prepared samples under shading from light for a few days after preparation.

Ex vivo CTL assay using the FACS-CTL assay

Next, an *ex vivo* CTL assay was done with the same protocol using spleen cells derived from virus-infected mice. Spleen cells were prepared from vSC-25-infected transgenic mice or normal BALB/c mice and used as effector cells for assays. As shown in Fig. 6, antigen-specific cytotoxic activities in spleen cells from infected mice could be determined by our assay with high sensitivity.

Determination of CTL activity against tumor cells

It is important to analyze the cytotoxic activities of CTLs against tumor cells. However, when tumor cells are used as sensitive targets, we often can not provide control targets for assays. Therefore, we tried to use calibration beads as a control for this assay. Because the fluorescent intensity of the calibration beads was strong, 15-12 cells were labeled with a low concentration of CFSE (final concentration at 50 nM) and incubated with various numbers of LINE-IIIB for 4 h at 37°C. After incubation, a 10 μL aliquot of diluted calibration beads was added to each sample and five thousand cells, which were contained in the gate consisting of region 1 (15-12 cells and beads) and two fluorescent peaks on a histogram plot (region 2; R2), were acquired. As shown in Fig. 7, even when calibration beads were used as a control for the assay, the cytotoxic activities of LINE-IIIB against 15-12 cells could be detected and the results obtained from the assay were in close agreement with the data obtained by using Neo as a control.

Table 1 Stability of prepared FACS-CTL assay samples

E/T ratio	% Specific Lysis		
	Day 0	Day 2	Day 3
5/1	10.9	11.0	17.0
10/1	29.4	31.7	33.6
20/1	46.5	52.5	52.3

4% paraformaldehyde-fixed samples were assessed just after preparation (day 0), and two days (day 2) and three days (day 3) after preparation by a FACScan analyzer. LINE-IIIB cells were used as effector cells. Percent specific lysis against P18-I10-pulsed P815 cells is shown.

DISCUSSION

In this paper, we reported a rapid and simple assay

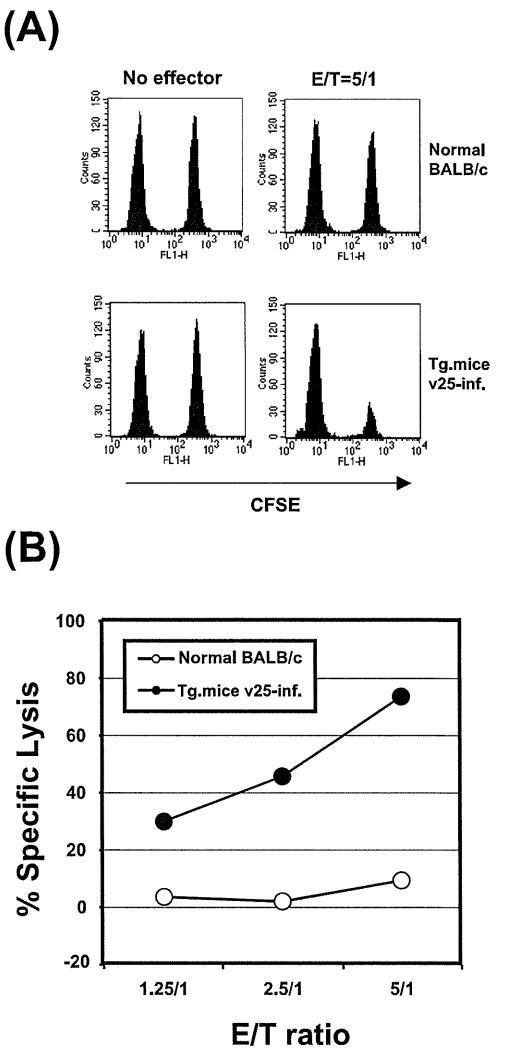

Fig. 6 Ex vivo CTL assay using the FACS-CTL assay. Tg-RT1 mice were intraperitoneally inoculated with 1×10^7 PFU of vSC-25. Seven days after inoculation, spleen cells were prepared from vSC-25-inoculated Tg-RT1 mice and from control normal BALB/c mice. Cytotoxic activities of these spleen cells were determined by FACS-CTL assay using peptide P18-I10-pulsed and unpulsed P815 cells as sensitive and control target cells, respectively. Histogram profiles (A) and percent specific lysis calculated by a formula (B) are shown.

to assess antigen-specific cytotoxic activities of CTLs *in vitro* using single fluorescent-dye CFSE. Recently, several flow cytometric assays to detect CTL activity using CFSE have been reported by others (5, 6, 8), but are still not widely used. From some of these reports, we can get more detailed information such as phenotyping of target cells or effector cell subsets other than specific cytotoxicity. However, these assays may not be easy to perform because they require several steps and complicated two-color dot blot analysis. Although it was possible to detect only the cytotoxic activity in our FACS-CTL assay, this assay is extremely simple; thus, it is suitable to quickly determine many samples similar to the ^{51}Cr-release assay. Moreover, with some improvements such as treatment with excess EDTA/trypsin reagents or using fluorescent calibration beads as a control, adherent cells and tumor cells also could be used as target cells. Although propidium iodide was not added to the samples to detect dead cells after incubation, it was not a problem in the analysis by our system because we always used target cells with high viability. Results obtained from this study suggest that the FACS-CTL assay is an acceptable alternative to the classical ^{51}Cr-release assay.

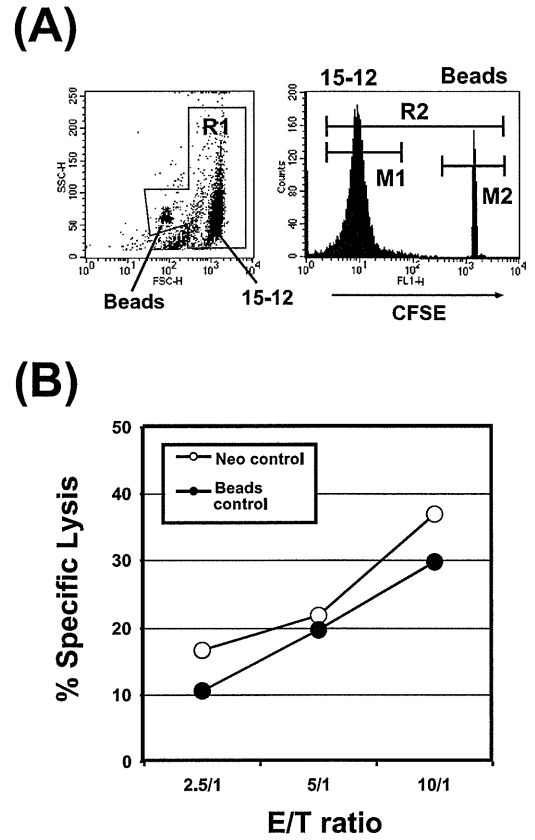

Fig. 7 FACS-CTL assay using fluorescent calibration beads as a control. (A) Gated region (R1) containing 50 nM of CFSE-labeled 15-12 cells and calibration beads on dot blot analysis and histogram profile of the cells in the gated region (R1) by FACScan analyzer are shown. For acquisition, 5×10^3 cells which were contained in both regions R1 and R2 were collected. (B) Cytotoxic activities of LINE-IIIB were determined by FACS-CTL assay using fluorescent calibration beads and 15-12 cells. 15-12 cells were labeled with 50 nM of CFSE and incubated with LINE-IIIB at various E/T ratios for 4 h at 37°C. After incubation, cells were treated with EDTA and trypsin solutions, washed with FACS buffer and resuspended with PFA-PBS. Ten µL aliquots of diluted calibration beads were added to each sample just before acquisition (closed symbols). For control experiments, cytotoxic activities of the same LINE-IIIB were determined using 2.5 µM of CFSE-labeled 15-12 cells and 50 nM of CFSE-labeled Neo were used as sensitive and control target cells, respectively (open symbols).

Furthermore, our FACS-CTL assay has some advantages over to the ^{51}Cr-release assay. First, in our assay, prepared samples are fixed with PFA, so samples with inherent risk such as virally infected cells can also be determined. Second, non-activating cells may be used as target cells. In the ^{51}Cr-release assay, resting cells or non-dividing cells such as murine naïve splenocytes (our unpublished observation) or neuronal cells do not easily incorporate ^{51}Cr and so it is difficult to use these cells as target cells. In contrast, these cells are labeled with CFSE the same as activating cells (1, 2, 9) because the CFSE reagent passively diffuses into these cells. We could also use these cells as targets in the FACS-CTL assay. Third, since the fluorescence of prepared samples is stable for as long as three days, it is possible to analyze samples with a FACScan analyzer even if they are stocked or transported from another area.

The FACS-CTL assay described in this study will allow precise quantitative measurement of cell-mediated cytotoxity and analysis of the fine mechanism of CTL function in the virological and immunological fields, including cancer research, and diverse situations in which laboratory restrictions exist concerning the use of radioisotopes.

Acknowledgements

This work was supported in part by grants from the Ministry of Education, Science, Sport, and Culture, from the Ministry of Health and Labor and Welfare, Japan, and from the Japanese Health Sciences Foundation, and by the Promotion and Mutual Aid Corporation for Private School of Japan.

REFERENCES

1. Barber DL, Wherry EJ and Ahmed R (2003) Cutting edge: rapid in vivo killing by memory CD8 T cells. *J Immunol* **171**, 27–31.
2. Byers AM, Kemball CC, Moser JM and Lukacher AE (2003) Cutting edge: rapid in vivo CTL activity by polyoma virus-specific effector and memory $CD8^+$ T cells. *J Immunol* **171**, 17–21.
3. Chang L, Gusewitch GA, Chritton DB, Folz JC, Lebeck LK and Nehlsen-Cannarella SL (1993) Rapid flow cytometric assay for the assessment of natural killer cell activity. *J Immunol Methods* **166**, 45–54.
4. Flieger D, Gruber R, Schlimok G, Reiter C, Pantel K and Riethmuller G (1995) A novel non-radioactive cellular cytotoxicity test based on the differential assessment of living and killed target and effector cells. *J Immunol Methods* **180**, 1–13.
5. Godoy-Ramirez K, Makitalo B, Thorstensson R, Sandstrom E, Biberfeld G and Gaines H (2005) A novel assay for assessment of HIV-specific cytotoxicity by multiparameter flow cytometry. *Cytometry A* **68**, 71–80.
6. Jedema I, van der Werff NM, Barge RM, Willemze R and Falkenburg JH (2004) New CFSE-based assay to determine susceptibility to lysis by cytotoxic T cells of leukemic precursor cells within a heterogeneous target cell population. *Blood* **103**, 2677–2682.
7. Karawajew L, Jung G, Wolf H, Micheel B and Ganzel K (1994) A flow cytometric long-term cytotoxicity assay. *J Immunol Methods* **177**, 119–130.
8. Lecoeur H, Fevrier M, Garcia S, Riviere Y and Gougeon ML (2001) A novel flow cytometric assay for quantitation and multiparametric characterization of cell-mediated cytotoxicity. *J Immunol Methods* **253**, 177–187.
9. Li X, Dancausse H, Grijalva I, Oliveira M and Levi AD (2003) Labeling Schwann cells with CFSE-an in vitro and in vivo study. *J Neurosci Methods* **125**, 83–91.
10. McGinnes K, Chapman G, Marks R and Penny R (1986) A fluorescence NK assay using flow cytometry. *J Immunol Methods* **86**, 7–15.
11. Papadopoulos NG, Dedoussis GV, Spanakos G, Gritzapis AD, Baxevanis CN and Papamichail M (1994) An improved fluorescence assay for the determination of lymphocyte-mediated cytotoxicity using flow cytometry. *J Immunol Methods* **177**, 101–111.
12. Takahashi H, Cohen J, Hosmalin A, Cease KB, Houghten R, Cornette JL, DeLisi C, Moss B, Germain RN and Berzofsky JA (1988) An immunodominant epitope of the human immunodeficiency virus envelope glycoprotein gp160 recognized by class I major histocompatibility complex molecule-restricted murine cytotoxic T lymphocytes. *Proc Natl Acad Sci U S A* **85**, 3105–3109.
13. Takahashi H, Houghten R, Putney SD, Margulies DH, Moss B, Germain RN and Berzofsky JA (1989) Structural requirements for class I MHC molecule-mediated antigen presentation and cytotoxic T cell recognition of an immunodominant determinant of the human immunodeficiency virus envelope protein. *J Exp Med* **170**, 2023–2035.
14. Takahashi H, Merli S, Putney SD, Houghten R, Moss B, Germain RN and Berzofsky JA (1989) A single amino acid interchange yields reciprocal CTL specificities for HIV-1 gp160. *Science* **246**, 118–121.
15. Takahashi H, Nakagawa Y, Pendleton CD, Houghten RA, Yokomuro K, Germain RN and Berzofsky JA (1992) Induction of broadly cross-reactive cytotoxic T cells recognizing an HIV-1 envelope determinant. *Science* **255**, 333–336.
16. Takeshita T, Takahashi H, Kozlowski S, Ahlers JD, Pendleton CD, Moore RL, Nakagawa Y, Yokomuro K, Fox BS, Margulies DH and Berzofsky JA (1995) Molecular analysis of the same HIV peptide functionally binding to both a class I and a class II MHC molecule. *J Immunol* **154**, 1973–1986.
17. Yokosuka T, Takase K, Suzuki M, Nakagawa Y, Taki S, Takahashi H, Fujisawa T, Arase H and Saito T (2002) Predominant role of T cell receptor (TCR)-alpha chain in forming preimmune TCR repertoire revealed by clonal TCR reconstitution system. *J Exp Med* **195**, 991–1001.

Human Immunology 72 (2011) 783-790

Contents lists available at SciVerse ScienceDirect

journal homepage: www.elsevier.com/locate/humimm

Induction of CD56$^+$ T cells after prolonged activation of T cells *in vitro:* A possible mechanism for CD4$^+$ T-cell depletion in acquired immune deficiency syndrome patients

Megumi Takahashi*, Jiro Matsumura, Shinichiro Inagaki, Hidemi Takahashi

Department of Microbiology and Immunology, Nippon Medical school, Tokyo, Japan

ARTICLE INFO

Article history:
Received 13 April 2011
Accepted 8 June 2011
Available online 7 July 2011

Keywords:
CD56$^+$ T cells
HIV-1
CD4$^+$ T cell depletion
Immune activation

ABSTRACT

The pathogenic mechanisms responsible for depletion of CD4$^+$ T cells in aquired immune deficiency syndrome (AIDS) are not fully understood. Systemic immune activation mediated by persistent infection of human immunodeficiency virus (HIV) seems to be one of the predictors of disease progression. We predicted that certain lymphocytes responsible for CD4$^+$ T-cell depletion could be induced in patients during prolonged activation of lymphocytes. Therefore, we have established an *in vitro* long-term culture system for peripheral blood mononuclear cells with PHA-P stimulation and Herpesvirus saimiri infection, and examined what types of cells having strong cytotoxic activity to be emerged under the activated conditions. We observed that percentage of CD56$^+$ T cells was gradually increased in cultures from 30 days after stimulation and exhibited a cytotoxic activity against both autologous and allogeneic targets. Interestingly, HIV-1 infection enhanced the susceptibility of CD4$^+$ T cells to their cytotoxic effectors, and CD4$^+$ T cells from HIV-1–infected individuals showed decreased survival rate in the presence of autologous CD56$^+$ T cells. These findings raised the possibility that induction of autoreactive CD56$^+$ T cells in consequence of immune activation might be contributed to the depletion of CD4$^+$ T cells in HIV-1–infected patients.

1. Introduction

The progressive depletion of CD4$^+$ T cells in human immunodeficiency virus (HIV) –infected patients is still a major fundamental and controversial question in acquired immunde deficiency syndrome (AIDS) research. HIV selectively infects and kills cells expressing the CD4 molecule on their surface, particularly T lymphocytes and cells of the monocyte/macrophage lineage. Direct killing of infected cells appears to contribute to the loss of CD4$^+$ T cells in primary HIV-1 infection [1,2]. However, the percentage of HIV-1–infected CD4$^+$ T cells is too small to account for the extensive depletion of T-helper cells in patients who are progressing to AIDS through chronic infection with HIV-1 [3,4]. Thus, several other mechanisms have been proposed to explain the deletion of CD4$^+$ T cells [5,6].

HIV infection leads to sustained immune activation and causes profound alterations in T-cell homeostasis [7]. HIV-infected patients display elevated expression of activation markers, such as CD38, CD25, and CD69, on CD4$^+$ and CD8$^+$ T cells. High levels of proinflammatory cytokines and chemokines, such as tumor necrosis factor–α (TNF-α), interleukin-6 (IL-6), interleukin-1β (IL-1β), and macrophage inflammatory protein (MIP-1) are also observed in both plasma and lymph nodes in these patients [8,9]. Although the actual mechanisms underlying such an immune activation remain unclear, higher T-cell activation levels are associated with CD4$^+$ T-cell depression in untreated patients independent of plasma HIV RNA [10,11].

Previously, it has been reported that HIV-1–infected individuals had circulating cytotoxic T cells that were cytotoxic for noninfected CD4$^+$ T cells, and it was suggested that autoimmune phenomena contributed to the depletion of CD4$^+$ T cells [12,13]. It is interesting which types of cells are induced in consequence of immune activation and exhibit cytotoxicity against autologous CD4$^+$ T cells. In most *in vitro* studies, effector cells were prepared from peripheral blood mononuclear cells (PBMC) stimulated with mitogen followed by short-time culture in the presence of cytokines. We wanted to find effector cells in activated PBMC without adding any specific cytokines as well as antigens after long-term culture, because the presence of cytokines and antigens result in cytokine dependent expansions or antigen specific T-cell responses, and chronic immune activation persist for long time after HIV-1 infection *in vivo*. Therefore, we have established an *in vitro* long-term culture system for PBMC in the absence of cytokines and examined what types of cells are induced under the activated culture condition.

We found that CD56$^+$ T cells were gradually increased from long-cultured PBMC at approximately 30 days after stimulation, and we observed their cytotoxic activities against various tumor

* Corresponding author.
E-mail address: megumi@nms.ac.jp (M. Takahashi).

0198-8859/11/$32.00 - see front matter © 2011 American Society for Histocompatibility and Immunogenetics. Published by Elsevier Inc. All rights reserved.
doi:10.1016/j.humimm.2011.06.001

cells in a non–major histocompatibility complex (MHC)–restricted manner as well as autologous cells. It should be noted that HIV-1 infection enhanced the susceptibility of $CD4^+$ T cells to be killed by $CD56^+$ T cells. Moreover, $CD56^+$ T cells from HIV-1–infected patients exhibited a potent cytotoxicity against autologous $CD4^+$ T cells by *in vitro* activation. Therefore, if such autoreactive $CD56^+$ T cells will be expanded in HIV-1–infected patients, both non–HIV-1–infected and infected $CD4^+$ T cells might be strongly killed and depleted. Thus, we presented here a possible involvement of $CD56^+$ T cells in the depletion of $CD4^+$ T cells in HIV-1 infection.

2. Subjects and methods

2.1. Preparation of cells

Blood samples were obtained from healthy donors and highly active antiretroviral therapy (HAART)–treated or untreated asymptomatic HIV-1–infected individuals with peripheral $CD4^+$ T lymphocytes counts of >300/μl. All subjects gave informed consent under a protocol approved by the Institutional Review Board of the Nippon Medical School. PBMC were purified over a Ficoll density gradient and stimulated with 10 μg/ml of phytohemagglutinin-P (PHA-P: Sigma-Aldrich, St. Louis, MO) for 24 hours and subsequently inoculated with the Herpesvirus saimiri (HVS) strain C-488; kindly provided by M. Yasukawa at moi 10. Stimulated PBMC were cultured with T-cell culture medium (CTM) [14], composed of RPMI 1640 medium supplemented with 2 mmol/l of L-glutamine, 1 mmol/l of sodium pyruvate, 0.1 mmol/l of nonessential amino acids, a mixture of vitamins, 1 mmol/l of HEPES, 100 U/ml of penicillin, 100 μg/ml of streptomycin, 50 μmol/l of 2-mercaptoethanol, and heat-inactivated 10% fetal calf serum (FCS). Approximately 50 days later, stimulated PBMC, termed long-cultured PBMC (LC-PBMC), were used as effector cells in cell-mediated cytotoxicity assays. MOLT-4, MOLT-4/HIV-1_{IIIB} (kindly provided by S. Harada), Jurkat, K562 cells were cultured in CTM. Human glioblastoma cells, A172 and A172-448 [15], were grown in Eagle's minimum essential medium (MEM) supplemented with 10% FCS, 100 U/ml of penicillin, and 100 μg/ml of streptomycin. To establish the HVS transformed T-cell line, PBMC were stimulated with PHA-P and infected with HVS at moi 0.1. Stimulated cells were cultured in CTM with 100 U/ml of IL-2 for more than 3 months.

2.2. Antibodies and flow-cytometric analysis

Cells were pelleted and resuspended at a concentration of $<5 \times 10^5$ cells in 50 μl of PBS with 0.1% NaN_3 and 1% human serum containing each monoclonal antibody (mAb). FITC- or PE-labeled mouse anti-human CD3, CD4, CD8, CD56, CD1d, γδ, and Fas mAb were purchased from BD Biosciences (San Diego, CA). APC-labeled mouse anti-human CD3 and PE-labeled mouse anti-human MICA/B mAb were purchased from Biolegend (San Diego, CA). FITC-labeled mouse anti-human Vα24 mAb was purchased from Beckman Coulter, Inc. (La Brea, CA). PE-labeled mouse anti-human ULBP-2 mAb was purchased from R&D Systems, Inc. (Minneapolis, MN). After 30 minutes' incubation with each antibody at 4°C, cells were washed and resuspended in PBS for analysis by FACScan (BD Biosciences). Neutralizing antibodies against Fas ligand and NKG2D were purchased from R&D Systems, and CD1d were obtained from BD Biosciences.

2.3. Cytotoxicity assay

Cytotoxicity was assessed in a standard 4-hour ^{51}Cr-release assay with ^{51}Cr-labeled targets at various E:T ratios in 96well, U-bottomed culture plates. After incubation, the plates were centrifuged, and 100 μl of cell-free supernatants was collected to measure the radioactivity using a γ-counter. The percentage of specific ^{51}Cr release was calculated as follows: (experimental release- − spontaneous release)/(maximum release- − spontaneous release) × 100. In our laboratory, we cannot perform the ^{51}Cr-release assay using HIV-1–infected cells because of the constraint of Infectious Diseases Control Law in Japan. Therefore, we have established a method to measure the cytotoxic activity by flow-cytometric analysis using carboxyfluorescein succinimidyl ester (CFSE; Life Technology Corporation, Carlsbad, CA) staining [16]. Target cells were labeled with 0.8 nmol/l CFSE to differentiate from effector cells. Effectors and targets were mixed at a ratio of 1:1 and incubated at 37°C for 24 hours. After incubation, cells were harvested and resuspended in 4% paraformaldehyde in PBS and then stored at 4°C in the dark before cytometry. Figure 1A shows the cell size and granularity profiles of target cell alone (upper) and co-culture of targets and effectors (lower). High fluorescence intensity of CFSE in target cells was indicated by R1 region (R1 gate), and viable cells were gated from nonviable cells by their distinct forward scatter (FSC) versus side scatter (SSC) (R2 gate). R1 and R2 gates were used for estimation of survival target cell number. The percentage of survival target cells was calculated as follows: (survival target cells in co-culture of targets and effectors)/(survival targets in target cell alone) × 100.

2.4. Cell purification or depletion

Cells were incubated with biotinylated monoclonal antibody for 5 minutes at room temperature and washed three times with PBS. The labeled cells were then further incubated with streptoavidin microbeads (Miltenyi Biotec, Bergisch Gladbach, Germany), followed by magnetic column selection or depletion, respectively. Biotynylated mouse anti-human CD4 and CD8 were purchased from BD Biosciences, and CD56 were obtained from Biolegend.

2.5. Granzyme B activity

Granzyme B activity was determined by granzyme B (GrB)–specific hydrolysis of substrates. A 180-μl volume of the reaction mixture (200 mmol/l acetyl-Ile-Glu–Pro–Asp-paranitroanilide in reaction buffer containing 50 mmol/l HEPES, pH 7.5, 10% sucrose, 0.05% 3-(3-cholamidepropyl)dimethylammonio-1-propanesulphonate (CHAPS), and 5 mmol/l dithiothreitol (DTT)) was added to 20 μl of cell lysates. The absorbance at 405 nm was measured after incubation for 24 hours at 37°C. Concentration of samples were determined using a standard curve with recombinant mouse GrB (Sigma-Aldrich, St. Louis, MO).

2.6. Detection of HVS DNA

DNA was isolated from LC-PBMC and HVS transformed T-cell line using Blood & Tissue Genome Mini (Viogene, Sunnyvale, CA). HVS genome was detected by polymerase chain reaction (PCR) using the following primers for the STP gene from HVS subgroup C strain 488 to generate a 783-bp fragment: 5′-CTCTAAGCA-CAGGGGCACA-3′ and 5′-CTACGCAGAAGTCGGAAGCC-3′.

2.7. Statistical analysis

Student's *t* test was used to determine the significance of differences in means. A *p* value of <0.05 was considered significant.

3. Results

3.1. Expression of cytotoxic activity in LC-PBMC

To examine which types of cells to be emerged *in vitro* cultures of PBMC under the activated conditions, we have established a unique *in vitro* long-term culture system for PBMC without adding any exogenous cytokines as well as specific antigens, as the treatments lead to initiation of cytokine production or antigen-specific T-cell responses. To carry out the experiments, we cultured PBMC stimulated with PHA-P and subsequently infected with HVS. HVS, an oncogenic tumor virus of New World monkeys, has been reported to infect and to immortalize human CD4 and CD8 T cells

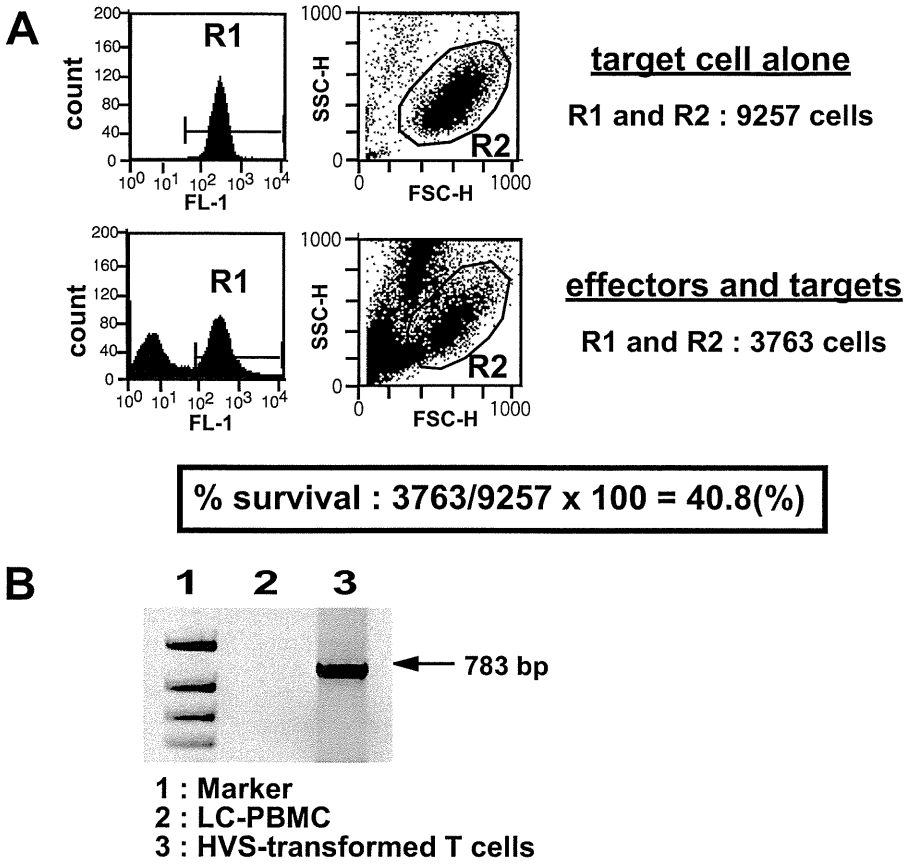

Fig. 1. Induction of long-cultured PBMC (LC-PBMC) and detection of their cytotoxic activity. (A) Method for measurement of cytotoxic activity by flow-cytometric analysis using carboxyfluorescein succinimidyl ester (CFSE) staining. R1, high fluorescence intensity of CFSE in target cells. R2, viable cells gated from nonviable cells by their distinct FSC versus SSC. A total of 10,000 cells gated in R1 were acquired, and R1 and R2 gates were used for estimation of survival target cell number. (B) PCR amplification of the Herpesvirus saimiri (HVS) genome. PCR products of the expected size were detected in HVS-infected owl monkey kidney cells and no PCR product was detected in LC-PBMC.

expressing $\alpha\beta$ and $\gamma\delta$ T cells [17,18]. We found that when PHA-stimulated PBMC were infected with HVS at high moi and then cultured in the absence of IL-2, T cells could maintain an activated state more than 30 days after stimulation. However, these treatments scarcely yielded HVS-transformed T-cells line. Indeed, as shown in Fig. 1B, we could not detect the PCR amplification of HVS gene in 60 days of cultured PBMC. We defined here such stimulated T cells as LC-PBMC, which could actively replicate more than 30 days after stimulation and maintain the cultures for more than 50 days without adding of any specific antigens and cytokines, but were not immortalized.

When we examined the cytotoxic potential of LC-PBMC after culturing them for more than 50 days in a ^{51}Cr -release cytotoxity assay, they showed significant killing activity against various T-cell lines, K562 cells, and A172 cells in a non–MHC-restricted manner. Moreover, LC-PBMC showed weak cytotoxicity against autologous PBMC (Fig. 2A). Next, we examined whether virus infection would affect the susceptibility to cytotoxic activity of LC-PBMC, by using persistently infected cell lines. Although MOLT-4 were efficiently killed by LC-PBMC, HIV-1-producing counterpart cells MOLT-4/HIV-1 were more sensitive to LC-PBMC. However, measles virus (MV)–infected A172-448 or HVS-transformed T cells were not susceptible compared with noninfected cells (Fig. 2B). These findings suggest that HIV-1 infection might enhance the susceptibility of infected cells to LC-PBMC.

3.2. $CD3^+CD56^+$ cells might be major effectors in LC-PBMC

We wanted to address the question of which types of cells among LC-PBMC are responsible for producing such cytotoxic activities. Therefore, aliquots of the cultures were removed on days 0, 3, 10, 20, 30, 40, and 50 of cultures for phenotypic analysis and measurement of cytotoxic activity against both MOLT-4 and MOLT-4/HIV-1. Time course analysis showed that until 30 days after, LC-PBMC exhibited little cytotoxic activity against both MOLT-4 and MOLT-4/HIV-1. However, after 40 days of stimulation, LC-PBMC mediated approximately 75% and 50% survival of MOLT-4 and MOLT-4/HIV-1, respectively, and another 10 days later LC-PBMC mediated less than 50% and 20% survival (Fig. 3A). The percentage of $CD3^-CD56^+$ cells was decreased by 20 days after *in vitro* stimulation, whereas that of $CD3^+CD56^+$ cells was increased gradually from 30 days after stimulation. Changes in the relative percentage of $\gamma\delta$T cells were minimal (Fig. 3B). These results suggested that $CD3^+CD56^+$ cells might be the major effectors in LC-PBMC, and natural killer (NK) cell and $\gamma\delta$ T-cell contribution was limited.

3.3. Characterization of cytotoxic cells in LC-PBMC

When the effector and target cells were separated by permeable filter, LC-PBMC showed minimal killing (data not shown). Therefore, cell–cell contact between effectors and targets are required for efficient killing by LC-PBMC. Figure 3 demonstrates that cytotoxic activity was elevated in parallel with increase of $CD3^+CD56^+$ cells. Thus, to examine the possible engagement of $CD3^+CD56^+$ cells in this cytotoxicity, $CD56^+$ cells were depleted from LC-PBMC by magnetic bead selection. An apparent reduction in cytotoxic activity was observed against MOLT-4/HIV-1 (Fig. 4A). In addition, depletion of $CD8^+$ cells had a significant effect on the cytotoxicity of LC-PBMC, as two-thirds of $CD3^+CD56^+$ cells were CD8 positive (Fig. 4B). Taken together, these results suggested that $CD3^+CD8^+CD56^+$

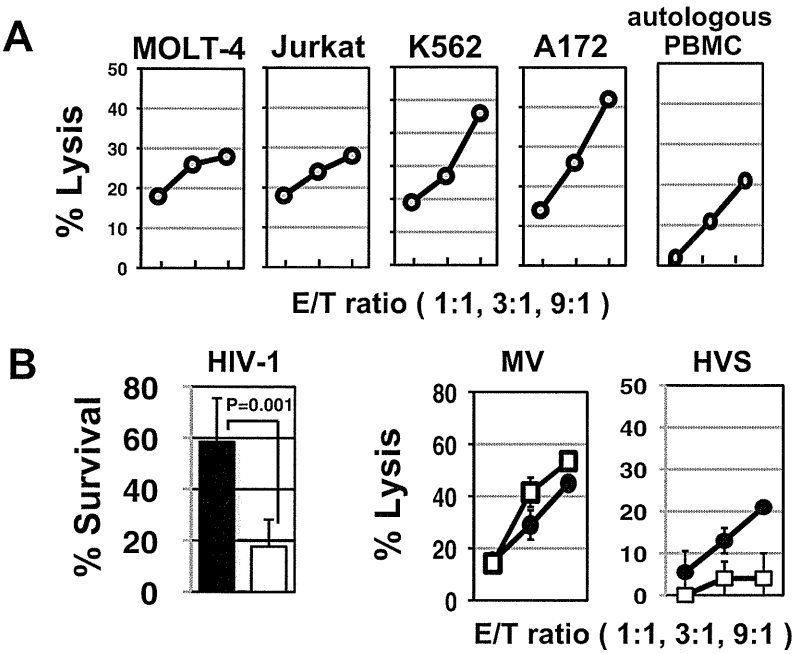

Fig. 2. Cytotoxic activity of long-cultured PBMC (LC-PBMC) against MOLT-4, Jurkat, K562, A172, and autologous PBMC (A). Cytotoxicity was assessed in ^{51}Cr-release assay. (B) Effect of virus infection on the susceptibility of target cells to cytotoxic activity of LC-PBMC. Assessment of cytotoxic activity was evaluated as survival rate in HIV-1 infection (closed bar; MOLT-4, open bar; MOLT-4/HIV-1) and was done as killing rate in measles virus (MV) (filled circle, A172; open square, A172-448) or Herpesvirus saimiri (HVS) infection (filled circle, PHA-P–stimulated T cells; open squares, HVS-transformed T cells).

cells might be the predominant effectors in LC-PBMC. We then assessed the contribution of FasL and NKG2D to LC-PBMC–mediated cytotoxicity using the neutralizing antibodies to FasL and NKG2D. Figure 4C demonstrates that anti-NKG2D antibody significantly affected the cytotoxic activity of LC-PBMC against MOLT-4/HIV-1, whereas anti-FasL antibody blocked the cytotoxicity only slightly. Moreover, increased granzyme B activity was observed when LC-PBMC were incubated with target cells (Fig. 4D).

Type 1 NKT cells is characterized by a semi-invariant T-cell receptor (TCR) using a unique TCR Vα24Jα18 chain in human and by its recognition of the glycolipid α-galactosylceramide (α-GalCer) loaded onto CD1d molecules. We tested the expression of Vα24 on CD3$^+$CD56$^+$ cells in LC-PBMC, but they did not express this molecule (Fig. 4E, left panel). We also examined whether cytotoxicity of target cells by LC-PBMC was in a CD1d-restricted manner, target cells were incubated with anti-CD1d neutralizing antibody [19] before co-culturing with effector cells. As shown in Fig. 4E, cytotoxic activity of LC-PBMC was not affected, suggesting that LC-PBMC-mediated cytotoxicity was not CD1d restricted.

3.4. HIV-1–infected CD4$^+$ T cells are more susceptible to cytotoxic activity of LC-PBMC

We then asked why HIV-1–infected cells are more susceptible to LC-PBMC–mediated killing than are noninfected cells. Because the killing of target cells was mostly NKG2D mediated, we examined the cell surface expression of ligands for NKG2D on both MOLT-4 and MOLT-4/HIV-1. Phenotypic analysis showed that the level of CD1d and MICA/B expression on MOLT-4/HIV-1 were lower than MOLT-4, whereas that of ULBP-2 was higher (Fig. 5A). These findings agree with previous report that HIV-1-Vpr up-regulated the expression of ligands for the activating NKG2D receptor, including ULBP-1, −2, and −3 but not MICA/B in infected cells [20]. However, as treatment of targets cells with anti–ULBP-2 antibody slightly blocked the cytotoxiciy of LC-PBMC (data not shown), all other ULBPs might be involved in enhancing susceptibility of HIV-1–infected cells to LC-PBMC–mediated killing.

Finally, to confirm the susceptibility of HIV-1–infected CD4$^+$ T cells to the cytotoxic activity of LC-PBMC, we infected primary CD4$^+$ T cells from healthy or HIV-1–infected donors with HIV-1 IIIB at moi of 0.1 for 4 days, followed by co-culturing with autologous LC-PBMC for 1 day. As shown in Fig. 5B, LC-PBMC were cytotoxic against autologous CD4$^+$ T cells and became more cytotoxic against HIV-1–infected CD4$^+$ T cells. Of note, although the percentages of CD3$^+$CD56$^+$ cells in LC-PBMC from HIV-1–infected individuals were little less than from healthy donors (data not show), CD4$^+$ T cells from HIV-1–infected patients showed a decreased survival rate in the presence of autologous LC-PBMC compared with healthy donors.

4. Discussion

Chronic immune activation is one of the characteristic features in HIV infection [21]. Polyclonal B-cell activation, increased T-cell turnover, increased frequencies of T cells with an activated phenotype, and increased serum levels of proinflammatory cytokines and chemokines were observed in HIV-1–infected patients [22]. In the absence of antiretroviral treatment, markers of T-cell activation and T-cell turnover predicted the rate of disease progression and CD4$^+$ T-cell depletion [10,23]. Chronic simian immunodeficiency virus (SIV) infection in macaques provides a relevant and useful model to explore the mechanisms for progressive CD4$^+$ T-cell decline in AIDS pathogenesis. Rhesus macaques, which develop progressive CD4$^+$ T-cell depletion and progression to AIDS upon SIV infection, are characterized by strong T-cell activation. In contrast, SIV-infected sooty mangabeys and African green monkeys, the natural hosts of SIV, which do not develop any immunodeficiency, exhibit minimal T-cell activation despite evident viral replication [24]. Although the underlying causes of immune activation have remained elusive, several mechanisms have been proposed. For example, CD4$^+$ T-cell depletion during the acute stage of HIV-1 infection occurs rapidly within the first few weeks of infection and is predominantly localized to the gastrointestinal tract. Therefore, in the context of a compromised gastrointestinal mucosal surface,

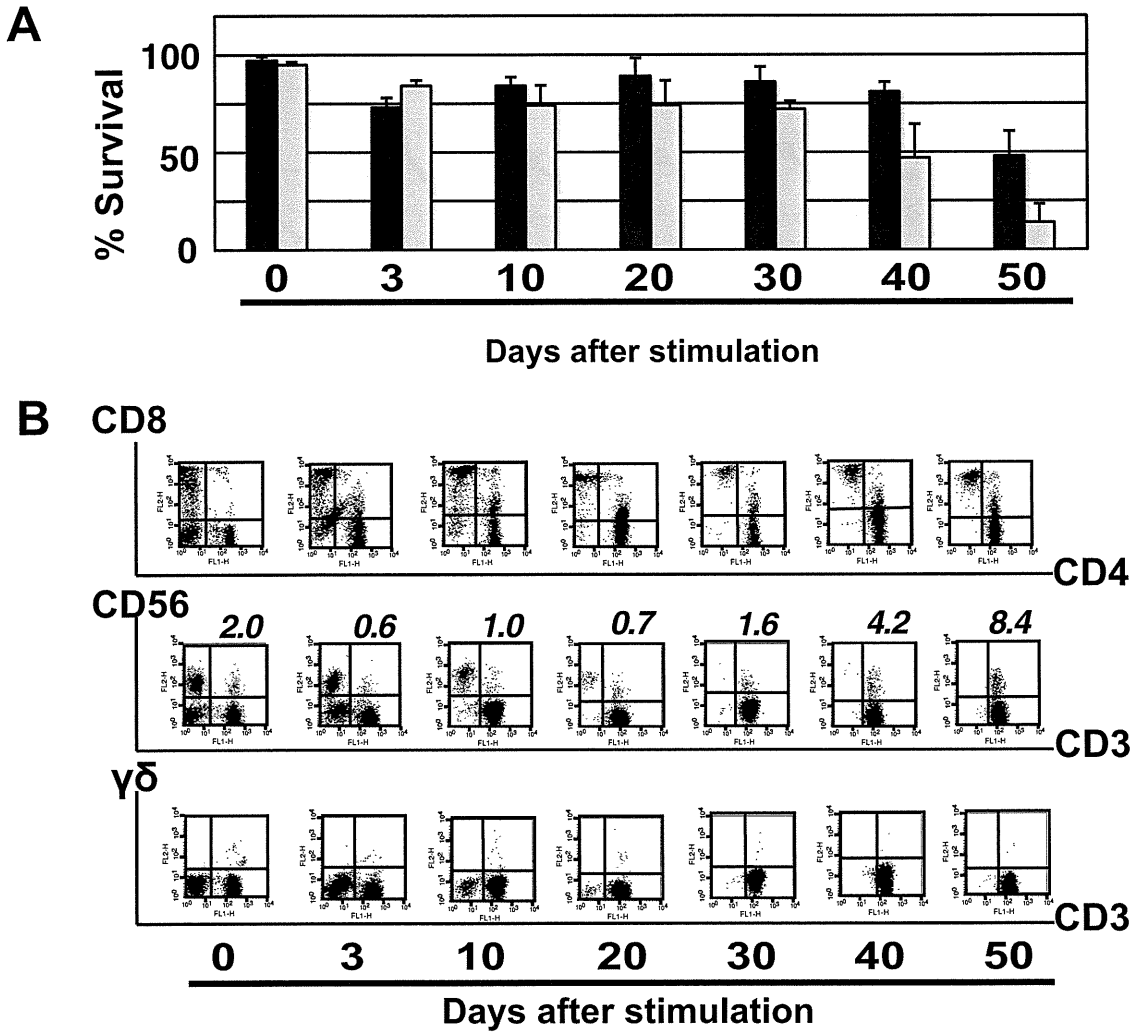

Fig. 3. $CD3^+CD56^+$ cells might be the major effectors in long-cultured PBMC (LC-PBMC). (A) Time course analysis of cytotoxic activity in LC-PBMC. PBMC were stimulated with PHA-P and subsequently infected with Herpesvirus saimiri (HVS). Aliquots of the cultures were removed on days 0, 3, 10, 20, 30, 40, and 50 of culture for measurement of cytotoxic activity against both MOLT-4 (filled bar) and MOLT-4/HIV-1 (open bar). Assessment of cytotoxic activity was evaluated as survival rate of target cells in triplicates (mean ± SD). (B) Time course analysis of phenotype in LC-PBMC. PBMC were stimulated with PHA-P and subsequently infected with HVS. Aliquots of the cultures were removed on days 0, 3, 10, 20, 30, 40, and 50 of culture for phenotypic analysis. The indicated numbers represent the percentages of $CD3^+CD56^+$ cells.

circulating microbial products (*e.g.*, lipopolysaccharide [LPS]) might be a possible cause of HIV-related systemic immune activation [25]. Furthermore, HIV-1 gene products such as gp120 or Nef are able to activate lymphocytes or to enhance their responsiveness to activation [26].

Activation of T cells includes their turnover, differentiation from naive to memory cells, and various type of cytokine production. These events might cause the alterations of constitution in immune cell populations. In this study, we applied an alternative approach using PHA-P and HVS infection to maintain an activated condition of T cells and examined which types of cells would emerge *in vitro* in cultures. We observed that $CD56^+$ T cells were gradually increased in the long-term culture conditions from 30 days after stimulation and exhibited a potent cytotoxic activity against both autologous and allogeneic targets. In human beings, innate and acquired immune responses are thought to be mediated in part by NK cells, γδ T cells, and T cells that express both NK cell–associated markers and TCR. Among NK-like T cells, $CD56^+$ T cells are well characterized for their phenotype and function [27–30]. $CD56^+$ T cells are a heterogeneous population that include $CD4^+$, $CD8^+$, and $CD4^-CD8^-$ cells expressing αβ or γδ TCR and various combinations of NK cell receptors. They account for a small percentage (~5%) of PBMC, but are present in remarkably high numbers in the liver and bone marrow of healthy adults, accounting for 15–55% of all T cells in these organs [31]. $CD56^+$ T cells possess dual innate and adaptive immune functions displaying properties of both T and NK cells capable of both MHC-restricted and non–MHC-restricted cytotoxicity and secretion of cytokines, including IFN-γ, TNF-α, and IL-4 [32]. These properties provide a role for $CD56^+$ T cells to regulate the immune responses against microorganisms and tumors. Indeed, decreased numbers of $CD56^+$ T cells have been reported to occur in the livers of chronically hepatitis C virus (HCV) –infected patients, and failure to eliminate HCV is thought to result from a deficiency of such innate lymphocytes [33,34].

Previous studies reported that invariant NKT (iNKT) cells, which comprise a small portion of peripheral $CD56^+$ T cells, expressing an invariant Vα24Vβ11 and recognizing glycolipid antigens presented by CD1d, were highly susceptible to HIV-1 infection, and that selective depletion of these cells might contribute to developments in HIV pathogenesis [35]. Because $CD56^+$ T cells observed in this study did not show the expression of Vα24 and CD1d-mediated cytotoxicity, they were not iNKT cells. There are few studies on the expres-

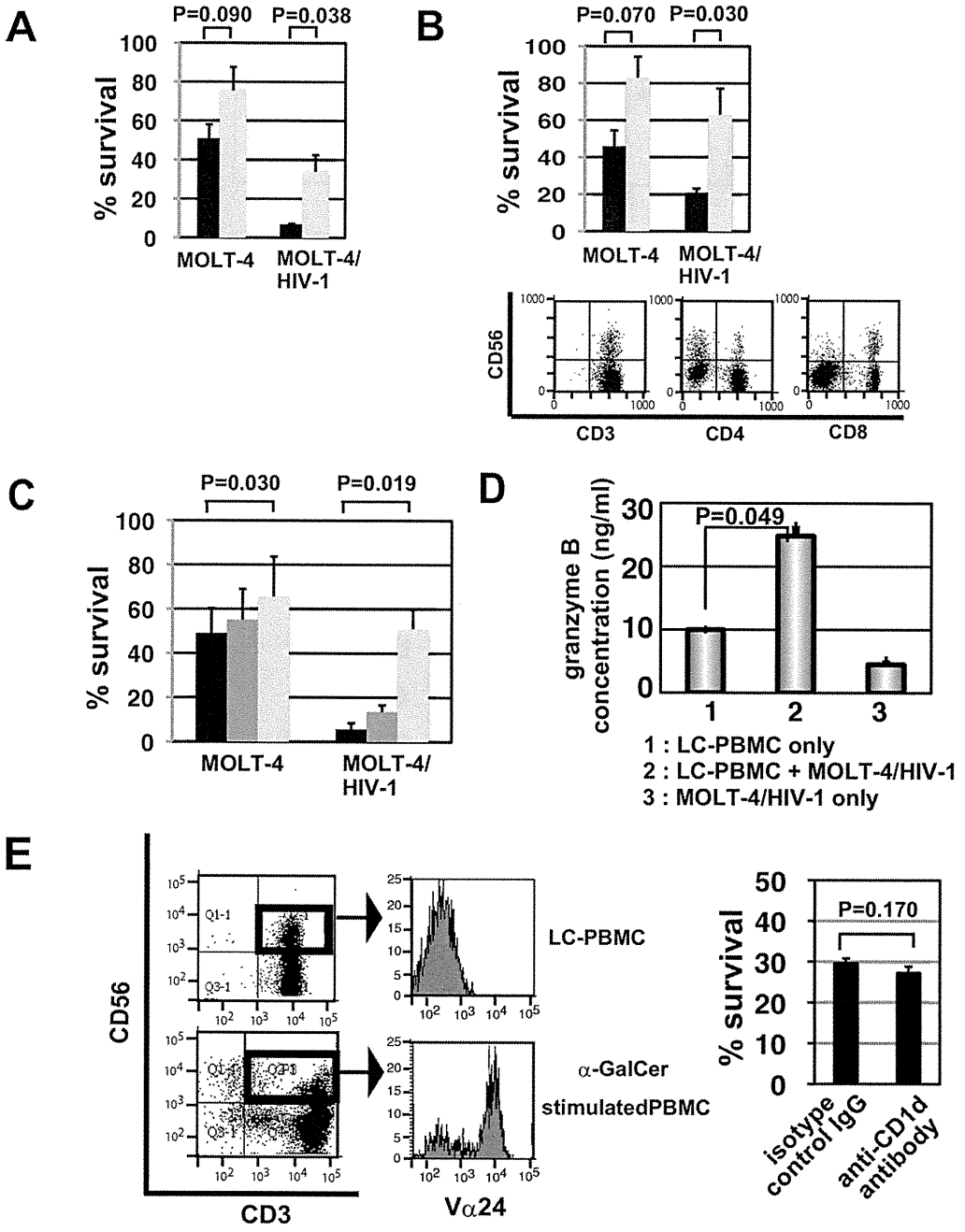

Fig. 4. Characterization of effector cells in long-cultured PBMC (LC-PBMC). Identification of effector cells in LC-PBMC. CD56$^+$ cells (A) or CD8$^+$ cells (B) were depleted from LC-PBMC by magnetic beads selection and subjected to cytotoxicity assay. (C) Effect of anti-FasL or NKG2D neutralizing antibody on cytotoxic activity of LC-PBMC. Effector cells and target cells were co-cultured in the presence of neutralizing antibodies and subjected to cytotoxicity assay. (A–C); Assessment of cytotoxic activity was evaluated as survival rate of target cells in triplicate (mean ± SD). (D) Granzyme B activity of LC-PBMC. LC-PBMC were cultured with or without MOLT-4/HIV-1. After 1 day, cells were harvested and subjected to measurement of granzyme B activity. (E) Examination of Vα24 expression on CD3$^+$CD56$^+$ cells. LC-PBMC and α-galactodemide stimulated PBMC were stained with APC (anti-CD3), PE, (anti-D56) and FITC (anti-Vα24) labeled antibodies (left panel). Target cells were incubated with anti-CD1d neutralizing antibody before coculturing with effector cells (right panel).

sion and function of CD56$^+$ T cells in HIV infection besides iNKT cells. Tarazona et al. observed a decreased number of CD8^{bright} T cells expressing CD56 in non–HAART-treated HIV-1 patients [36]. Parsons et al. reported that the phenotypic changes of CD56 from positive to negative on CD8$^+$ T cells with non–MHC-restricted cytotoxicity occurred in progressive HIV infection, and suggested that these changes might reflect autoreactive and pathogenic diversion of the CD8$^+$ T-cell repertoire [37].

Induction of CD56$^+$ T cells by PHA-P stimulation and HVS infection do not necessarily reflect cytotoxic T cells *in vivo*. However, when we examined the cytotoxic activity of CD56$^+$ T cells from HIV-1–infected or noninfected donors, CD56$^+$ T cells were cytotoxic against autologous CD4$^+$ T cells and became more cytotoxic against HIV-1–infected CD4$^+$ T cells. It should be noted that CD4$^+$ T cells from HIV-1–infected patients showed significant susceptibility against autologous CD56$^+$ T cells. The percentages of CD3$^+$CD56$^+$ cells in LC-PBMC from HIV-1–infected patients were little less than from healthy donors. These findings suggest that CD56$^+$ T cells from HIV-1–infected patients are more likely to acquire a potent cytotoxicity under the activated culture condition.

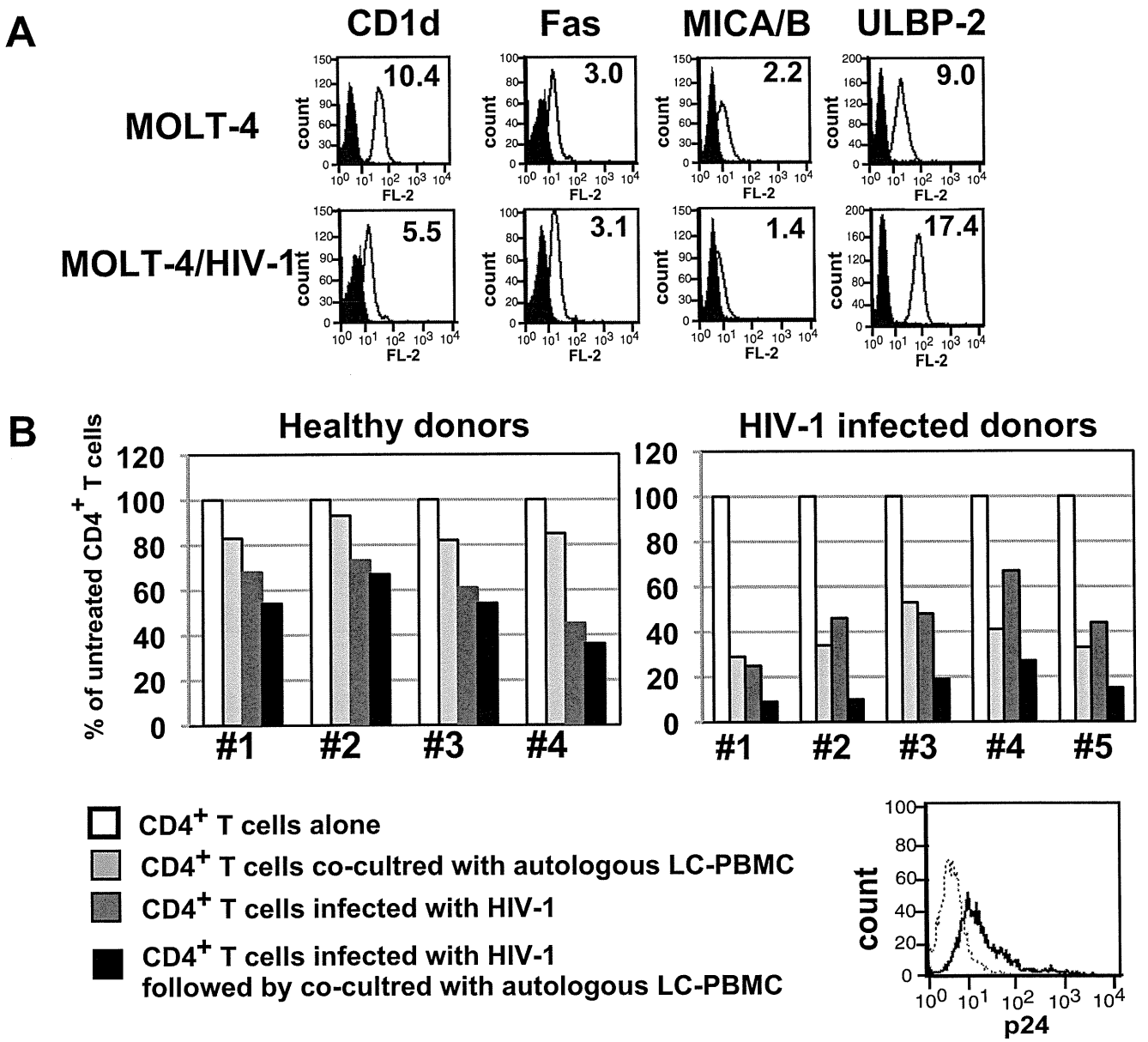

Fig. 5. $CD4^+$ T cells from HIV-1-infected individuals are more susceptible to cytotoxic activity of autologous long-cultured PBMC (LC-PBMC). (A) Cell surface expression of ligands for NKG2D on both MOLT-4 and MOLT-4/HIV-1. Both cells were stained with anti-CD1d, Fas, MICA/B, or ULBP-2 antidody. MFI values are indicated in the upper right corner of histogram. (B) Enhancement of susceptibility of $CD4^+$ T cells against autologous LC-PBMC by HIV-1 infection. PBMC from healthy and HIV-1-infected donors were stimulated with PHA-P followed by HVS infection. After ~50 days' incubation, cells were harvested and used as LC-PBMC. $CD4^+$T cells were purified from PHA-P-stimulated PBMC by magnetic beads selection and infected with HIV-1 IIIB at 0.1 moi for 4 days, and then co-cultured with autologous LC-PBMC for 1 day. Assessment of cytotoxic activity was evaluated as survival rate of target cells. HIV-1 infection was confirmed by intracellular staining of HIV-1 gag antigen p24. Results were normalized and are expressed as percentages of intact $CD4^+$ T cells.

We assumed that if the level of immune activation was highly elevated, autoreactive $CD56^+$ T cells might be up-regulated and expanded in HIV-1-infected patients. Therefore, we present here our findings on the possible involvement of $CD56^+$ T cells in the depletion of $CD4^+$ T cells.

Some HIV-1-infected individuals have autoreactive antibodies directed CD4 molecules, human leukocyte antigen (HLA) class II, and myelin basic protein [38,39]. Recently Kuwata et al. demonstrated that increased autoreactive antibodies correlated with the extent of $CD4^+$ T-cell depletion in an SIV/macaque model [40]. Induction and development of autoreactive antibodies is also likely to be caused by immune activation in HIV-1-infected patients. Therefore, it is necessary to block or to minimize immune activation and inflammation to prevent such unfavorable responses. Antiretroviral therapy exerts a suppressive effect on T-cell activation and apoptosis through its potent and prolonged inhibition of HIV replication. However, there are several limitations to application of HIV therapy for HIV-1-infected individuals, such as drug resistance and dose-limiting side effects. Use of immunosuppressive agents or inhibitors of proinflammatory cytokines might also be effective for suppression of immune activation. However, because the immune system also has to cope with other persisting or exogenous pathogens, casual use of these agents may cause progression toward severe infectious disease. Therefore, a better understanding of the mechanisms by which HIV-1 infection causes immune activation is required for the development of strategies for control of immune activation, that is, what types of agents we can use, or under what conditions these agents can be used.

References

[1] Brenchley JM, Schacker TW, Ruff LE, et al. CD4+ T-cell depletion during all stages of HIV disease occurs predominantly in the gastrointestinal tract. J Exp Med 2004;200:749-59.

[2] Mehandru S, Poles MA, Tenner-Racz K, et al. Primary HIV-1 infection is associated with preferential depletion of CD4+ T lymphocytes from effector sites in the gastrointestinal tract. J Exp Med 2004;200:761-70.

[3] Harper ME, Marselle LM, Gallo RC, Wong-Staal F. Detection of lymphocytes expressing human T-lymphotropic virus type III in lymph nodes and peripheral blood from infected individuals by in situ hybridization. Proc Natl Acad Sci U S A 1986;83:772-6.

[4] Schnittman SM, Psallidopoulos MC, Lane HC, et al. The reservoir for HIV-1 in human peripheral blood is a T-cell that maintains expression of CD4. Science 1989;245:305-8.

[5] Gougeon ML, Piacentini M. New insights on the role of apoptosis and autophagy in HIV pathogenesis. Apoptosis 2009;14:501-8.

[6] Herbeuval JP, Grivel JC, Boasso A, et al. CD4+ T-cell death induced by infectious and noninfectious HIV-1: Role of type 1 interferon-dependent, TRAIL/DR5-mediated apoptosis. Blood 2005;106:3524-31.

[7] Hazenberg MD, Stuart JW, Otto SA, Borleffs JC, Boucher CA, de Boer RJ, et al. T-cell division in human immunodeficiency virus (HIV)-1 infection is mainly due to immune activation: A longitudinal analysis in patients before and during highly active antiretroviral therapy (HAART). Blood 2000;95:249-55.

[8] Hazenberg MD, Otto SA, van Benthem BH, et al. Persistent immune activation in HIV-1 infection is associated with progression to AIDS. AIDS 2003;17:1881-8.

[9] Lederman MM, Kalish LA, Asmuth D, Fiebig E, Mileno M, Busch MP. "Modeling" relationships among HIV-1 replication, immune activation and CD4+ T-cell losses using adjusted correlative analyses. AIDS 2000;14:951-8.

[10] Deeks SG, Kitchen CM, Liu L, et al. Immune activation set point during early HIV infection predicts subsequent CD4+ T-cell changes independent of viral load. Blood 2004;104:942-7.

[11] Hunt PW, Brenchley J, Sinclair E, et al. Relationship between T-cell activation and CD4+ T-cell count in HIV-seropositive individuals with undetectable plasma HIV RNA levels in the absence of therapy. J Infect Dis 2008;197:126-33.

[12] Zarling JM, Ledbetter JA, Sias J, Fultz P, Eichberg J, Gjerset G, et al. HIV-infected humans, but not chimpanzees, have circulating cytotoxic T lymphocytes that lyse noninfected CD4+ cells. J Immunol 1990;144:2992-8.

[13] Grant MD, Smaill FM, Rosenthal KL. Lysis of CD4+ lymphocytes by non-HLA-restricted cytotoxic T lymphocytes from HIV-infected individuals. Clin Exp Immunol 1993;93:356-62.

[14] Takahashi M, Osono E, Nakagawa Y, Wang J, Berzofsky JA, Margulies DH, et al. Rapid induction of apoptosis in CD8+ HIV-1 envelope-specific murine CTLs by short exposure to antigenic peptide. J Immunol 2002;169:6588-93.

[15] Takahashi M, Watari E, Shinya E, Shimizu T, Takahashi H. Suppression of virus replication via down-modulation of mitochondrial short chain enoyl-CoA hydratase in human glioblastoma cells. Antivir Res 2007;75:152-8.

[16] Nakagawa Y, Watari E, Shimizu M, Takahashi H. One-step simple assay to determine antigen-specific cytotoxic activities by single-color flow cytometry. Biomed Res 2011; 32:159-66.

[17] Yasukawa M, Inoue Y, Kimura N, Fujita S. Immortalization of human T cells expressing T-cell receptor gamma delta by Herpesvirus saimiri. J Virol 1995;69:8114-7.

[18] Takahashi M, Ido E, Uesaka H, Fukushima T, Ibuki K, Miura T, et al. Comparison of susceptibility to SIVmac239 infection between CD4+ and CD4+ 8+ T cells. Arch Virol 2005;150:1517-28.

[19] Galli G, Nuti S, Tavarini S, Galli-Stampino L, De Lalla C, Casorati G, et al. CD1d-restricted help to B cells by human invariant natural killer T lymphocytes. J Exp Med 2003;197:1051-7.

[20] Richard J, Sindhu S, Pham TN, Belzile JP, Cohen EA. HIV-1 Vpr up-regulates expression of ligands for the activating NKG2D receptor and promotes NK cell-mediated killing. Blood 2010;115:1354-63.

[21] Appay V, Sauce D. Immune activation and inflammation in HIV-1 infection: Causes and consequences. J Pathol 2008;214:231-41.

[22] Biancotto A, Grivel JC, Iglehart SJ, et al. Abnormal activation and cytokine spectra in lymph nodes of people chronically infected with HIV-1. Blood 2007;109:4272-9.

[23] Giorgi JV, Lyles RH, Matud JL, et al. Predictive value of immunologic and virologic markers after long or short duration of HIV-1 infection. J Acquir Immune Defic Syndr 2002;29:346-55.

[24] Silvestri G, Sodora DL, Koup RA, Paiardini M, O'Neil SP, McClure HM, et al. Nonpathogenic SIV infection of sooty mangabeys is characterized by limited bystander immunopathology despite chronic high-level viremia. Immunity 2003;18:441-52.

[25] Brenchley JM, Price DA, Schacker TW, et al. Microbial translocation is a cause of systemic immune activation in chronic HIV infection. Nat Med 2006;12:1365-71.

[26] Manninen A, Renkema GH, Saksela K. Synergistic activation of NFAT by HIV-1 nef and the Ras/MAPK pathway. J Biol Chem 2000;275:16513-7.

[27] Mingari MC, Vitale C, Cambiaggi A, Schiavetti F, Melioli G, Ferrini S, et al. Cytolytic T lymphocytes displaying natural killer (NK)-like activity: Expression of NK-related functional receptors for HLA class I molecules (p58 and CD94) and inhibitory effect on the TCR-mediated target cell lysis or lymphokine production. Int Immunol 1995;7:697-703.

[28] Norris S, Doherty DG, Collins C, McEntee G, Traynor O, Hegarty JE, et al. Natural T cells in the human liver: Cytotoxic lymphocytes with dual T-cell and natural killer cell phenotype and function are phenotypically heterogenous and include Valpha24-JalphaQ and gammadelta T-cell receptor bearing cells. Hum Immunol 1999;60:20-31.

[29] Campbell JJ, Qin S, Unutmaz D, Soler D, Murphy KE, Hodge MR, et al. Unique subpopulations of CD56+ NK and NK-T peripheral blood lymphocytes identified by chemokine receptor expression repertoire. J Immunol 2001;166:6477-82.

[30] Linn YC, Hui KM. Cytokine-induced NK-like T cells: From bench to bedside. J Biomed Biotechnol 2010 2010;2010:435745.

[31] Doherty DG, O'Farrelly C. Innate and adaptive lymphoid cells in the human liver. Immunol Rev 2000;174:5-20.

[32] Kelly-Rogers J, Madrigal-Estebas L, O'Connor T, Doherty DG. Activation-induced expression of CD56 by T cells is associated with a reprogramming of cytolytic activity and cytokine secretion profile in vitro. Hum Immunol 2006;67:863-73.

[33] Golden-Mason L, Madrigal-Estebas L, McGrath E, Conroy MJ, Ryan EJ, Hegarty JE, et al. Altered natural killer cell subset distributions in resolved and persistent hepatitis C virus infection following single source exposure. Gut 2008;57:1121-8.

[34] Deignan T, Curry MP, Doherty DG, Golden-Mason L, Volkov Y, Norris S, et al. Decrease in hepatic, CD56+ T cells and V alpha CD24+ natural killer T cells in chronic hepatitis C viral infection. J Hepatol 2002;37:101-8.

[35] Li D, Xu XN. NKT cells in HIV-1 infection. Cell Res 2008;18:817-22.

[36] Tarazona R, DelaRosa O, Casado JG, Torre-Cisneros J, Villanueva JL, Galiani MD, et al. NK-associated receptors on CD8 T cells from treatment-naive HIV-infected individuals: Defective expression of CD56. AIDS 2002;16:197-200.

[37] Parsons MS, Zipperlen K, Gallant M, Howley C, Grant M. Distinct phenotype of unrestricted cytotoxic T lymphocytes from human immunodeficiency virus-infected individuals. J Clin Immunol;30:272-9.

[38] Thiriart C, Goudsmit J, Schellekens P, Barin F, Zagury D, De Wilde M, et al. Antibodies to soluble CD4 in HIV-1-infected individuals. AIDS 1988;2:345-51.

[39] Mathiesen T, Sönnerborg A, Wahren B. Detection of antibodies against myelin basic protein and increased levels of HIV-IgG antibodies and HIV antigen after solubilization of immune complexes in sera and CSF of HIV infected patients. Viral Immunol 1989;2:1-9.

[40] Kuwata T, Nishimura Y, Whitted S, et al. Association of progressive CD4+ T-cell decline in SIV infection with the induction of autoreactive antibodies. PLoS Pathog 2009;5;e1000372.

INFECTION AND IMMUNITY, Dec. 2011, p. 4791–4801 Vol. 79, No. 12
0019-9567/11/$12.00 doi:10.1128/IAI.05808-11

Production of Autoantibodies by Murine B-1a Cells Stimulated with *Helicobacter pylori* Urease through Toll-Like Receptor 2 Signaling▽†

Fumiko Kobayashi,[1,2] Eri Watanabe,[1] Yohko Nakagawa,[1] Shingo Yamanishi,[1] Yoshihiko Norose,[1] Yoshitaka Fukunaga,[2] and Hidemi Takahashi[1]*

Department of Microbiology and Immunology[1] and Department of Pediatrics,[2] Nippon Medical School, Tokyo 113-8602, Japan

Received 16 August 2011/Accepted 18 September 2011

***Helicobacter pylori* infection is associated with several autoimmune diseases, in which autoantibody-producing B cells must be activated. Among these B cells, CD5-positive B-1a cells from BALB/c mice were confirmed to secrete autoantibodies when cocultured with purified *H. pylori* urease in the absence of T cells. To determine the mechanisms for autoantibody production, CD5-positive B-1a cells were sorted from murine spleen cells and stimulated with either purified *H. pylori* urease or *H. pylori* coated onto plates (referred to hereafter as plate-coated *H. pylori*), and autoantibody production was measured by enzyme-linked immunosorbent assay (ELISA). Complete urease was not secreted from *H. pylori* but was visually expressed over the bacterium-like endotoxin. Urease-positive plated-coated *H. pylori* stimulated B-1a cells to produce autoantibodies, although urease-deficient isotype-matched *H. pylori* did not. Autoantibody secretion by B-1a cells was inhibited when bacteria were pretreated with anti-*H. pylori* urease-specific antibody having neutralizing ability against urease enzymatic activity but not with anti-*H. pylori* urease-specific antibody without neutralizing capacity. The B-1a cells externally express various Toll-like receptors (TLRs): TLR1, TLR2, TLR4, and TLR6. Among the TLRs, blocking of TLR2 on B-1a cells with a specific monoclonal antibody (MAb), T2.5, inhibited autoantibody secretion when B-1a cells were stimulated with plate-coated *H. pylori* or *H. pylori* urease. Moreover, B-1a cells from TLR2-knockout mice did not produce those autoantibodies. The present study provides evidence that functional urease expressed on the surface of *H. pylori* will directly stimulate B-1a cells via innate TLR2 to produce various autoantibodies and may induce autoimmune disorders.**

Helicobacter pylori causes not only a variety of gastroduodenal diseases but also various autoimmune disorders, such as rheumatoid arthritis (RA) (16), idiopathic thrombocytopenic purpura (ITP) (7), and Sjogren's syndrome (SjS) (3); however, the actual underlying relationship between *H. pylori* infection and the induction of autoimmune diseases remains unknown.

The relationship between pathogen intrusion and the induction of autoimmune disorders has been defined over the last decade; for example, infection of BALB/c mice with either coxsackievirus or murine cytomegalovirus results in the development of myocarditis and the production of autoantibodies to cardiac myosin from 28 days after infection (25). Thus, T cells and autoantibodies specific for the pathogens in the acquired immunity have been thought to be critical for the induction of autoimmune disorders; however, in some cases, infectious viruses, the causative agents, cannot be detected after 14 days of infection and actual evidence of molecular mimicry in the development of myocarditis has not been confirmed (5). This strongly indicates that the nonspecific adjuvant effect (2) derived from pathogens and damaged self-components produced via infection may persistently stimulate innate immune responses to progress chronic autoimmune disorders. These innate immune cells generally do not respond to specific antigenic epitopes on pathogens but do react against pathogen-associated molecular patterns (PAMPs) via pattern recognition receptors, such as Toll-like receptors (TLRs). Thus, autoimmunity accompanied by the production of various autoantibodies is possibly elicited through continual stimulation of innate TLRs by some PAMPs of pathogens causing chronic infection.

In our previous study, we found that purified urease isolated from *H. pylori* activated murine B cells to produce various autoantibodies, such as immunoglobulin M (IgM)-type rheumatoid factor (RF IgM), anti-single-stranded DNA antibody, and antiphosphatidylcholine (anti-PC) antibody, in a T-cell-independent manner (33). Moreover, as expected, B cells able to be stimulated by *H. pylori* urease are $CD5^+$ innate B-1a cells that predominantly secrete IgA-, IgM-, and IgG3-type antibodies. In contrast to T-cell-dependent B-2 cells in the acquired arm, T-cell-independent innate B-1a cells mainly localize in the peritoneal and pleural cavities or mucosal compartments so that they may come into direct contact with *H. pylori* at the gastric mucosa.

In the present study, we found that urease is not actively secreted from *H. pylori* but, rather, is expressed on the surface of spiral-shaped bacteria and that urease-positive *H. pylori*-coated plates appear to stimulate purified $CD5^+$ B-1a cells to produce various autoantibodies, although urease-deficient bacteria do not. Moreover, autoantibody secretion by B-1a cells was apparently inhibited when bacterium-coated plates were pretreated with anti-*H. pylori* urease-specific antibody. In this

* Corresponding author. Mailing address: Department of Microbiology and Immunology, Nippon Medical School, 1-1-5 Sendagi, Bunkyo-ku, Tokyo 113-8602, Japan. Phone: 81 3 3822 2131, ext. 5381. Fax: 81 3 3316 1904. E-mail: htkuhkai@nms.ac.jp.

▽ Published ahead of print on 26 September 2011.

† The authors have paid a fee to allow immediate free access to this article.

case, antibodies that could abrogate the enzymatic activity of bacterial urease, such as UB-33-specific antibodies (14), showed an inhibitory ability. Furthermore, blocking of TLR2 on B-1a cells with a specific monoclonal antibody (MAb), T2.5 (19), significantly inhibited the secretion of autoantibodies when stimulated with *H. pylori*-coated urease-positive plates. This was confirmed by using B-1a cells from TLR2-knockout mice.

These findings indicate that the functional urease expressed on the surface of *H. pylori* directly stimulates TLR2 on innate B-1a cells in the gastric mucosa to produce various autoantibodies like PAMPs and may induce autoimmune disorders.

MATERIALS AND METHODS

Animals. Six- to 8-week-old female BALB/c mice and 10-week-old female Japanese white rabbits were purchased from Nisseizai (Tokyo, Japan), and 6-week-old female TLR2-knockout ($TLR2^{-/-}$) BALB/c mice (29) were purchased from Oriental Bioservice (Kyoto, Japan). These animals were maintained in microisolator cages under pathogen-free conditions and fed autoclaved laboratory chow and water. All animal experiments were performed according to the guidelines of the National Research Council *Guide for the Care and Use of Laboratory Animals* (22a) and approved by the Review Board of Nippon Medical School.

Bacterial strains and growth conditions. The bacteria used in the present study were two known wild-type *H. pylori* strains, Sydney strain 1 (SS-1) (17) and NCTC 11637 (4). To obtain a large amount of bacterial cells, we used the following methods, as described previously (8). In brief, either the SS-1 or NCTC 11637 isolate was cultured on brucella agar (BD Biosciences, San Diego, CA) containing 5% horse serum (Sigma-Aldrich, St. Louis, MO) and 1% β-cyclodextrin (Wako Junyaku, Osaka, Japan) at 37°C under microaerophilic conditions (5% O_2, 15% CO_2, and 80% N_2) with an AnaeroPack sachet (MicroAero; Mitsubishi Gas Chemical, Tokyo, Japan). After a 2-day culture, the colonies were harvested by scraping with a sterile metal spatula, transferred to 50 ml brucella broth (BD Biosciences) containing 5% horse serum and 1% β-cyclodextrin, and further cultured for 24 h at 37°C. Then, 500 μl cell-containing medium was plated on brucella agar for an additional 3 days at 37°C, and the grown bacterial cells were harvested and washed with cold phosphate-buffered saline (PBS) at pH 7.0. The cells were sedimented by centrifugation (10,000 × *g* for 10 min at 4°C), and the cell pellet was stored at −80°C. A urease-negative mutant of *H. pylori*, HPP1801, which originated from the NCTC 11637 isolate (32), a kind gift from Tomoko Mizote at Yamaguchi Prefectural University, was cultured on brucella broth containing 5% horse serum, 1% β-cyclodextrin, and 10 μg/ml kanamycin (Wako Junyaku).

Purification of *H. pylori* urease. *H. pylori* urease was purified biochemically as described previously (33). Briefly, the stored cell pellet containing about 1 g *H. pylori* cells was thawed and vortexed with sterile distilled water. The cells were removed from the mixture by centrifugation, and the supernatant was filtered with a 0.22-μm-pore-size filter (Millipore, Billerica, MA) to obtain water extract. Then, the column containing Cellufine sulfate (Millipore) was equilibrated with PE65 buffer (20 mM phosphate buffer [PB] and 1 mM EDTA at pH 6.5). About 6.5 ml of prepared water extract was then applied to the column and eluted with the PE65 buffer. Urease-containing fractions were harvested by measuring enzyme activity, adjusted to pH 5.5, and adsorbed to the second-step column that had been preequilibrated with an another buffer, termed PO55 (20 mM PB at pH 5.5), for washing. Gel-bound urease was also eluted using PO74 buffer (20 mM PB and 0.15 M NaCl at pH 7.4). Each eluted fraction was analyzed for its enzyme activity quantitatively, and the positive fractions were collected in a single tube. For the collected sample, it was confirmed whether it contained *H. pylori* urease by Western blot analysis, as described below. The purity of the eluted urease was examined by silver staining using a silver staining kit (Wako Junyaku), and the purified urease protein concentration was estimated using a Micro BCA protein assay reagent kit (Pierce Co., Inc., Rockford, IL).

Western blotting for *H. pylori* urease. Samples were loaded onto a sodium dodecyl sulfate (SDS)-polyacrylamide gel for electrophoresis and then transferred to a nitrocellulose-polyvinylidene difluoride membrane (Atto, Tokyo, Japan) using blotting buffer (2 M Tris [pH 8.0], 1.43% glycine, 5% methanol). The blots were blocked overnight at 4°C with Block Ace (Dainihon Seiyaku, Osaka, Japan). The membrane was incubated with anti-whole *H. pylori* urease-specific antibody from immune rabbit serum and two murine *H. pylori* urease-specific MAbs, termed L2 for the large subunit (UreB) (22) and S2 for the small subunit (UreA) (15). The blots were washed five times with PBS containing 0.05% Tween 20 (T-PBS) and incubated with biotinylated goat anti-rabbit immunoglobulin (Ig) and anti-mouse Ig (Vector Laboratories, Burlingame, CA) at 1:200 in PBS for 2 h at room temperature (RT). After being washed three times, the blots were incubated with streptavidin-alkaline phosphatase (Nichirei, Tokyo, Japan) diluted 1:5 in PBS for 30 min at RT. Then, the blots were detected with a ProtoBlot nitroblue tetrazolium and 5-bromo-4-chloro-3-indolylphosphate color development system (Promega Corporation, Madison, WI).

Purification of *H. pylori* lipopolysaccharide (LPS). Cells were lysed in Tris HCl (pH 6.8) containing 2% SDS at 90°C for 10 min. Protein content was measured using the BCA protein assay reagent kit. Samples of cell lysates were adjusted to equal protein contents (1 mg/ml) and then proteolyzed in reaction mixtures containing Tris HCl, SDS, and proteinase K at 60°C for 2 h. The proteolyzed samples were extracted with hot phenol, mixed with equal volumes of water and phenol, and incubated at 70°C with repeated vortexing for 20 min. After centrifugation at 12,000 × *g* for 15 min at 10°C, the aqueous phases were collected. The phenolic phases were reextracted with 1 volume of H_2O at 70°C for 10 min, and the centrifugation was repeated. The combined aqueous extracts were adjusted to 0.5 M NaCl, precipitated with 10 volumes of ethanol in the refrigerator overnight, and then centrifuged at 20,000 × *g* for 20 min at 10°C and air dried.

Electrophoretic analyses of *H. pylori* LPS. Samples were applied to a 15% polyacrylamide separating gel containing 3.2 M urea and a 5% stacking gel. After electrophoresis at 25 mA for 90 min, the gel was either fixed for silver staining (30) or transferred to a polyvinylidene difluoride membrane using blotting buffer (20). Primary antibody, monoclonal anti-Lewis x (Le^x; clone P12 [21]; Signet, Dedham, MA) or anti-Lewis y (Le^y; 1:100; clone F3 [21]; Signet), and secondary antibody (biotinylated goat anti-mouse IgM; 1:1,000; BD Bioscience) were diluted in PBS containing 0.5% bovine serum albumin (BSA) (13). Then, streptavidin peroxidase (Nichirei) was diluted 1:5 in PBS. The blots were detected with a tetramethylbenzidine (TMB) development system (Vector Laboratories, Burlingame, CA).

Preparation of anti-*H. pylori* urease-specific antibodies. Anti-*H. pylori* urease-specific antibodies were obtained from rabbits immunized with either purified urease or synthetic peptides purchased from Takara Bio (Tokyo, Japan). To induce the neutralizing antibody that abrogates the enzymatic activity of *H. pylori* urease, a 19-mer peptide, UB-33 (amino acids 321 to 339 [CHHLDKSIKEDV QFADSRI]), from a large subunit of *H. pylori* urease (UreB) (14) was administered intramuscularly into rabbits with the same volume of complete Freund adjuvant. At 2 and 8 weeks after immunization, rabbits were boosted with UB33 peptide mixed with the same volume of incomplete Freund adjuvant. Antibody-containing serum was collected 3 weeks after the last immunization and purified using a protein A column (GE Healthcare, Uppsala, Sweden).

Detection of *H. pylori* urease in growth medium. A 100-μl aliquot of the known *H. pylori* urease-specific MAb L2 (5 μg/ml) (14) was added to 96-well flat-bottom plates (Thermo Fisher Scientific, Roskilde, Denmark), and the mixture was incubated overnight at 4°C. After incubation, antibody-coated plates were blocked with PBS containing 1% BSA for 3 h at RT and washed twice with T-PBS. A 50-μl aliquot of sample was added, and 50 μl diluted anti-whole urease rabbit serum (1:200) was added. After washing with T-PBS, 50 μl diluted peroxidase-conjugated goat antirabbit antibody (Rockland, Gilbertsville, PA) was added, the mixture was incubated with 50 μl TMB-soluble reagent (Scy-Tek Laboratories, Logan, UT) for 20 min, and 50 μl TMB stopping solution (Scy-Tek Laboratories) was added. The color changes were quantitated by measurement of the absorbance at 450 nm with a microplate reader (Bio-Rad, Hercules, CA).

Immunohistological staining for *H. pylori* urease and LPS. Cultured *H. pylori* was plated on a micro-slide glass and fixed with 4% paraformaldehyde (PFA)-PBS (pH 7.2) for 30 min at RT. In the light microscopic view, after washing with PBS, blocking solution (PBS containing 1% BSA and 0.3% normal goat serum) was added to the micro-slide glass and incubated for 1 h. After washing with PBS, anti-urease-specific rabbit serum was added and the mixture was incubated for an additional 1.5 h. Then, biotinylated goat antirabbit antibody (Dako, Glostrup, Denmark) was added for 1 h and the mixture was incubated with streptavidin complex (ABC complex kit; Vector Laboratories) for 20 min. After washing with PBS, diaminobenzidine (DAB; Vector Laboratories) was added and the reaction was stopped with distilled water.

As for *H. pylori* LPS staining, either monoclonal anti-Lewis x (clone P12) or anti-Lewis y (clone F3) (1:40) was added and the mixture was incubated at 37°C for 2 h. After washing with PBS, secondary antibody (biotinylated goat anti-mouse IgM, 1:200) was added, and the mixture was incubated for an additional 1 h and then further incubated with streptavidin complex (ABC complex kit; Vector Laboratories) for 30 min. After washing with PBS, DAB (Vector Laboratories) was added and the reaction was stopped with distilled water. In electron

microscopic analysis, fixed *H. pylori* cells were embedded in a 1% agarose gel, which was then cut into thin sections (1 to 2 mm^3) and stained with anti-urease-specific rabbit serum. The stained block was fixed with 2.5% glutaraldehyde–0.1 M PB (pH 7.3) and 1% osmium tetroxide–0.1 M PB. Then, the sample was dehydrated with a series of graded ethanol and polymerized with Epon 812 resin (TAAB Laboratories, Berks, United Kingdom). Thin sections were made using an ultramicrotome (Leica, Solms, Germany), and the sections were stained with lead citrate and observed with an electron microscope (JEOL-1010; Nihon Denshi, Tokyo, Japan).

Purification and sorting of B-1a cell subset. After red blood cells had been depleted with ammonium chloride, the remaining splenic lymphocytes or peritoneal cavity-derived cells from mice were incubated with anti-Thy1.2 MAb (Serotec Ltd., Oxford, United Kingdom), followed by the addition of rabbit complement (Cederane, Ontario, Canada) at 37°C for 1 h to deplete T lymphocytes as described previously (28). Live cells were harvested and confirmed to be B cells of >90% purity by flow cytometry (BD Bioscience) using fluorescein isothiocyanate (FITC)-conjugated rat anti-mouse B220 MAb (RA3-6B2; PharMingen, San Diego, CA). Purified B cells were incubated in 200 μl RPMI 1640-based culture medium (CM) containing 10% heat-inactivated fetal calf serum (FCS), 20 mM HEPES (Gibco BRL, Grand Island, NY), 10 mM 2-mercaptoethanol (Sigma-Aldrich), 100 U/ml penicillin, 0.1 mg/ml streptomycin, and 10 μg/ml gentamicin at 37°C in a 5% CO_2 atmosphere on 96-well U-bottom plates (BD Falcon, Franklin Lakes, NJ). To obtain a B-1a ($B220^+/CD5^+$) or B-2 ($B220^+/CD5^-$) cell subset, purified splenic B cells were further sorted using a FACSAria-II cell sorter (BD Bioscience) and FITC-conjugated rat anti-mouse B220 MAb and phycoerythrin (PE)-conjugated anti-mouse CD5 MAb (53-7.3; PharMingen). Sorted cells were confirmed to be either B-1a or B-2 cells of >90% purity. In some experiments, we used peritoneal cavity-derived B-1a cells (perC B-1a cells), obtained by flushing the peritoneal cavity with RPMI 1640 supplemented with 10% FCS and 1 mM EDTA. perC B-1a cells were isolated using a two-step process. First, macrophages were depleted with two successive pannings of adherent cells for 2 h at 37°C in 5% CO_2, followed by depletion of T cells with antibodies to the pan-T-cell marker Thy1.2 with Dynabeads according to the manufacturer's instructions (Dynal Biotech, Oslo, Norway). The purified cells were 92% $B220^+$ $CD5^+$ B-1a cells. However, we could always obtain fewer perC B-1a cells than sorted splenic B-1a cells from a mouse. Thus, we used sorted splenic B-1a cells for further experiments.

Enzyme-linked immunosorbent assay (ELISA). Purified B cells, B-1a cells, or B-2 cells either were added to *H. pylori* coated onto plates (referred to hereafter as plate-coated *H. pylori*) or cultured with 10 μg/ml purified *H. pylori* urease or PBS for 7 days *in vitro*, and the culture supernatants were harvested and analyzed. All the experiments were performed in triplicate.

Detection of IgG3. A 50-μl aliquot of affinity-purified rabbit anti-mouse IgG3 (10 μg/ml in PBS; Rockland) was added and the mixture was incubated at 4°C. After overnight incubation, the antigen-coated plates were blocked with BSA in PBS, and then 50 μl cultured supernatant was plated for an additional 60 min. After washing with T-PBS, 50 μl diluted biotinylated goat anti-mouse Ig (1:5,000; Amersham Bioscience) was added for 60 min, followed by horseradish peroxidase-avidin D (1:2,000; Vector Laboratories). After washing with T-PBS, 50 μl TMB staining solution was added, the mixture was incubated for 20 min, and a 100-μl aliquot of TMB stopping solution was added. The changes were quantitated by measurement of the absorbance at 450 nm with a microplate reader. On the basis of the mouse reference serum for standard IgG3 (Bethyl Laboratories, Inc., Montgomery, TX), we determined the concentration of serum IgG3.

Detection of ssDNA. Stock solution containing calf thymus DNA (type I; 1 mg/ml in H_2O; Sigma-Aldrich) was boiled for 10 min in a 1/10 volume of 1 N NaOH. The boiled solution was immediately put on ice for 10 min and diluted to 3 μg/ml with cold borate-buffered saline. A 100-μl aliquot of prepared single-stranded DNA (ssDNA) was added and blocked with 0.5% BSA and 0.04% Tween 20 in borate-buffered saline (BBT). A 50-μl aliquot of diluted (1:10) culture supernatant was incubated overnight at 4°C, a 50-μl aliquot of diluted biotinylated goat anti-mouse Ig (1:5,000) was added, and bound Ig was detected with a similar procedure. On the basis of the mouse reference serum for standard anti-ssDNA MAb (clone F7-26; Millipore), we determined the concentration of anti-ssDNA.

Detection of PC. A 100-μl aliquot of L-α-phosphatidylcholine from frozen egg yolk (type XIII-E; 50 μg/ml in ethanol; Sigma-Aldrich) was added to the plates, and the plates were incubated overnight at 4°C. After blocking, a 50-μl aliquot of the culture supernatant was plated, followed by biotinylated goat anti-mouse Ig, and bound Ig was measured with a similar procedure.

Detection of RF IgM. RF IgM was detected with an RF IgM (mouse) ELISA kit (Shibayagi, Gunma, Japan). According to the manufacturer's procedure, IgM type RF was measured.

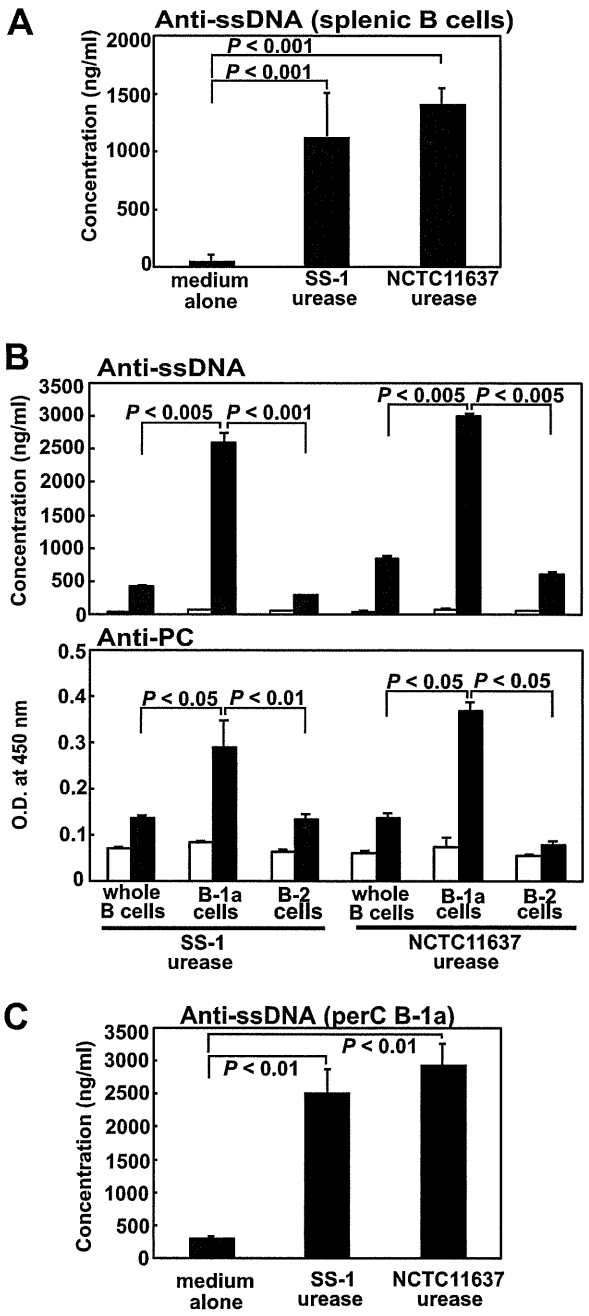

FIG. 1. Autoantibody secretion from purified murine splenic B cells as well as their sorted B-1 or B-2 cells stimulated with purified *H. pylori* urease. (A) Purified B cells (1×10^6) were cultured with 10 μg/ml purified *H. pylori* urease from either the SS-1 or NCTC 11637 isolate for 7 days, and the supernatants were harvested to measure their anti-ssDNA autoantibody production by ELISA. Data are means ± SDs ($n = 6$). (B) Either 2×10^5 purified B cells or the same number of their sorted B-1a or B-2 cells were cultured with 10 μg/ml purified *H. pylori* urease (filled columns) or PBS (open columns) for 7 days in CM, and the supernatants were harvested to measure either their anti-ssDNA (top) or anti-PC (bottom) autoantibody production. Data are means ± SDs ($n = 6$). O.D., optical density. (C) Purified peritoneal cavity-derived B-1a (perC B-1a) cells (1×10^5) were cultured with 10 μg/ml purified *H. pylori* urease for 7 days, and the supernatants were harvested to measure their anti-ssDNA autoantibody production. Statistical significance was determined by the Student *t* test, and the values are given in each graph.

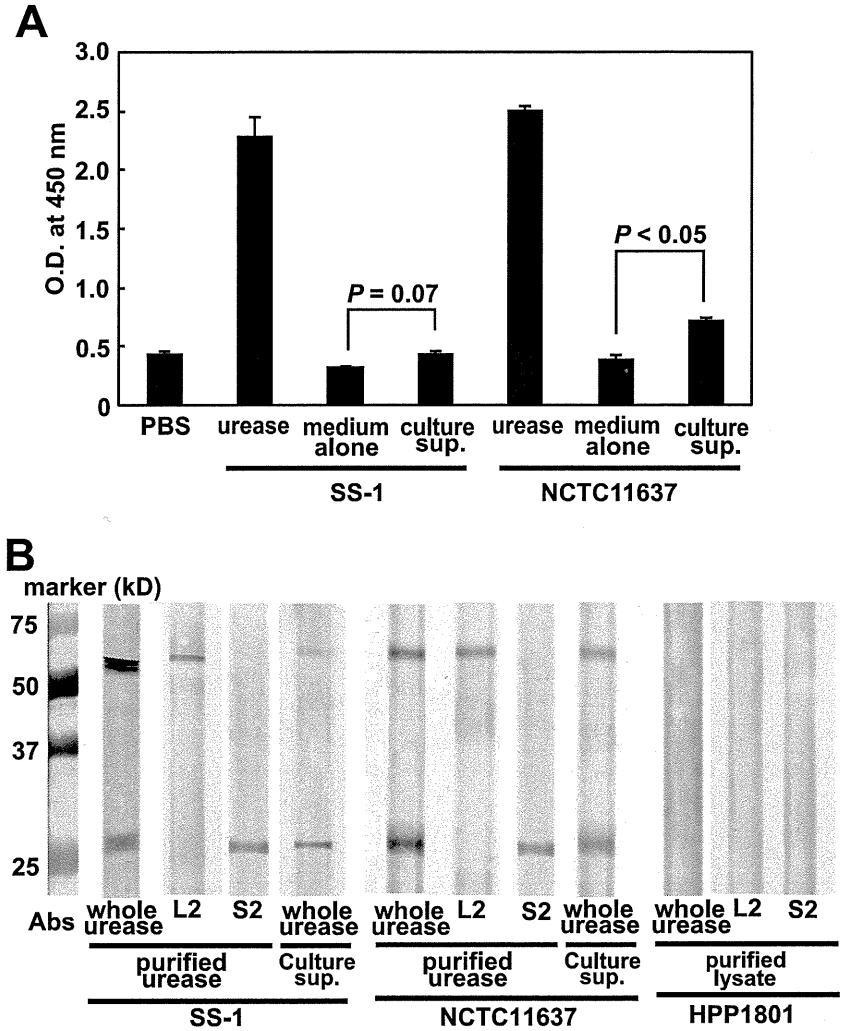

FIG. 2. Detection of *H. pylori* urease in the bacterial culture supernatant by sensitive ELISA using *H. pylori* urease-specific MAb. (A) Urease-positive *H. pylori* strains (isolates SS-1 and NCTC 11637) were cultured in brucella broth containing 5% horse serum for 2 days, and cell-free culture supernatant (culture sup.) was collected carefully and further sedimented by centrifugation (3,000 rpm for 5 min at 4°C) to remove debris. Compared with positive controls containing purified *H. pylori* urease (100 μg/ml), *H. pylori* urease was only slightly detected in the bacterial culture supernatant. Results are expressed as means ± SDs ($n = 5$). Statistical significance was determined by the Student t test, and the values are given in the graph. (B) We then tried to confirm the results by Western blotting by using whole urease-specific antibody from immune rabbit sera and two *H. pylori* urease-specific MAbs, L2 for the large subunit (UreB) and S2 for the small subunit (UreA), as described in Materials and Methods. We could detect both the large subunit (UreB) and the small subunit (UreA) in the culture supernatants of both SS-1 and NCTC 11637 compared with purified urease obtained from the bacteria. We have confirmed that HPP1801, a urease-negative mutant from the NCTC 11637 isolate, did not express urease in its lysates.

Coating of culture plates with *H. pylori*. The grown *H. pylori* cells were harvested and sedimented by centrifugation (3,000 × *g* for 10 min). The cell pellet was adjusted to a McFarland index 2 standard with PBS. For fixation, the same volume of 2% PFA solution was added to the pellet, and the mixture was incubated for 10 min at 10°C (9). Then, a 100-μl aliquot of PFA-fixed *H. pylori* was further incubated for 40 min at 60°C for plate coating.

Blocking of urease on the surface of *H. pylori* with specific rabbit antibodies. After coating 96-well round-bottom plates with *H. pylori*, 50 μg diluted (1:200) antibodies for *H. pylori* urease (anti-whole urease antibody, anti-UB-33 antibody) was added to each well, the plates were incubated at 37°C for 90 min, and the cells were washed three times with CM.

Effect of antibodies on *H. pylori* urease activity. To investigate the inhibitory effect of antibodies on the enzymatic activity of *H. pylori* urease, the urease (0.2 μg in 50 μl of 20 mM PB, pH 6.8) was mixed with purified antibody in 96-well plates. The mixture was incubated for 90 min. After incubation, 100 μl of reacted solution was mixed with 100 μl of 100 mM Sorensen's PB (pH 6.8) containing 100 mM urea (Wako) and 0.005% phenol red (Wako). Using a microreader, the time course of the color development was monitored by measurement of the absorbance at 540 nm at 60-min intervals for 7 h.

Detection of TLRs by reverse transcription-PCR analysis. Total RNA was extracted from 3×10^5 cells of each cell preparation using a commercial RNeasy kit (Qiagen, Hilden, Germany). Transcripts of TLRs as well as the housekeeping gene glyceraldehyde-3-phosphate (GAPDH) were amplified by PCR. The primer sets used to perform the PCR analysis are shown in Fig. 6A. After 35 cycles of PCR, the PCR products were resolved by electrophoresis in agarose gels and visualized by ethidium bromide staining using a UV light source.

Flow cytometric analysis of TLRs on B-1a cells. Purified B-1a cells were stained with the following anti-mouse TLR-specific rat antibodies and PE-conjugated goat anti-rat IgG (clone 405406; BioLegend, San Diego, CA) and analyzed by flow cytometry: anti-mouse TLR1 antibody (clone TR23; eBioscience, San Diego, CA), anti-mouse TLR2 antibody (clone 6C2; eBioscience) (23), anti-mouse TLR3 antibody (clone T3.7C3; eBioscience), anti-mouse TLR4/MD-2 antibody (clone MTS510; eBioscience), and anti-mouse TLR6 antibody (clone 41861; R&D Systems Inc., Minneapolis, MN). B-1a cells were also stained

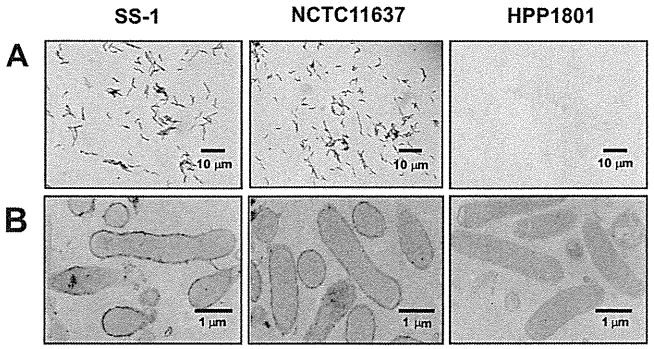

FIG. 3. Detection of *H. pylori* urease on/in the bacteria by immunohistological staining using murine *H. pylori* urease-specific antibody. *H. pylori* urease-positive isolates (SS-1 and NCTC 11637) and an *H. pylori* urease-negative isolate (HPP1801) were used for staining. Immunohistological analysis to detect the localization of *H. pylori* urease was carried out using light microscopy (magnification, ×800) (A) and electron microscopy (magnification, ×15,000) (B).

with either PE-conjugated anti-mouse TLR7 antibody (polyclonal; Imgenex, San Diego, CA), PE-conjugated anti-mouse TLR8 antibody (clone 44C143; Imgenex), or FITC-conjugated anti-mouse TLR9 antibody (clone M9.D6; eBioscience).

Blocking of cell surface TLRs on B-1a cells. Purified murine B-1a cells were incubated with anti-mouse TLR1 antibody, anti-mouse TLR2 (clone T2.5; eBioscience) (19), anti-mouse TLR4/MD-2 antibody, anti-mouse TLR6 antibody, or anti-mouse IgG1 isotype control (clone 11711; R&D Systems) (final concentration, 1 μg/10^6 cells) for 30 min at 37°C. After incubation, cells were washed three times with CM and added to round-bottom 96-well plates.

Statistical analysis. The results were analyzed using Student's *t* test, and the results are presented as means ± standard deviations (SDs). Differences at *P* values of <0.05 were considered significant.

RESULTS

Secretion of anti-ssDNA-specific autoantibody by purified murine B-1a cells stimulated with purified *H. pylori* urease. We have reported previously that murine B cells, in particular, $CD5^+$ B-1a cells, secreted various autoantibodies, such as IgM-type RF, anti-ssDNA-specific antibody, and anti-PC-specific antibody, when stimulated with purified *H. pylori* urease *in vitro* (33). Here, we confirmed the production of anti-ssDNA-specific autoantibody by enriched murine splenic B cells stimulated with purified *H. pylori* urease from either isolate SS-1 or isolate NCTC 11637 (Fig. 1A). We observed similar results in autoantibody production against ssDNA and PC when sorted splenic $CD5^+$ B-1a cells but not $CD5^{--}$ B-2 cells were stimulated with purified *H. pylori* urease (Fig. 1B). These findings indicate that among B cells, murine B-1a cells are the actual targets for *H. pylori* urease. We have seen similar results by using murine B-1a cells obtained from the peritoneal cavity (perC B-1a) (Fig. 1C). Thus, there seems to be no difference between splenic B-1a cells and perC B-1a cells in the response against purified *H. pylori* urease to produce autoantibodies.

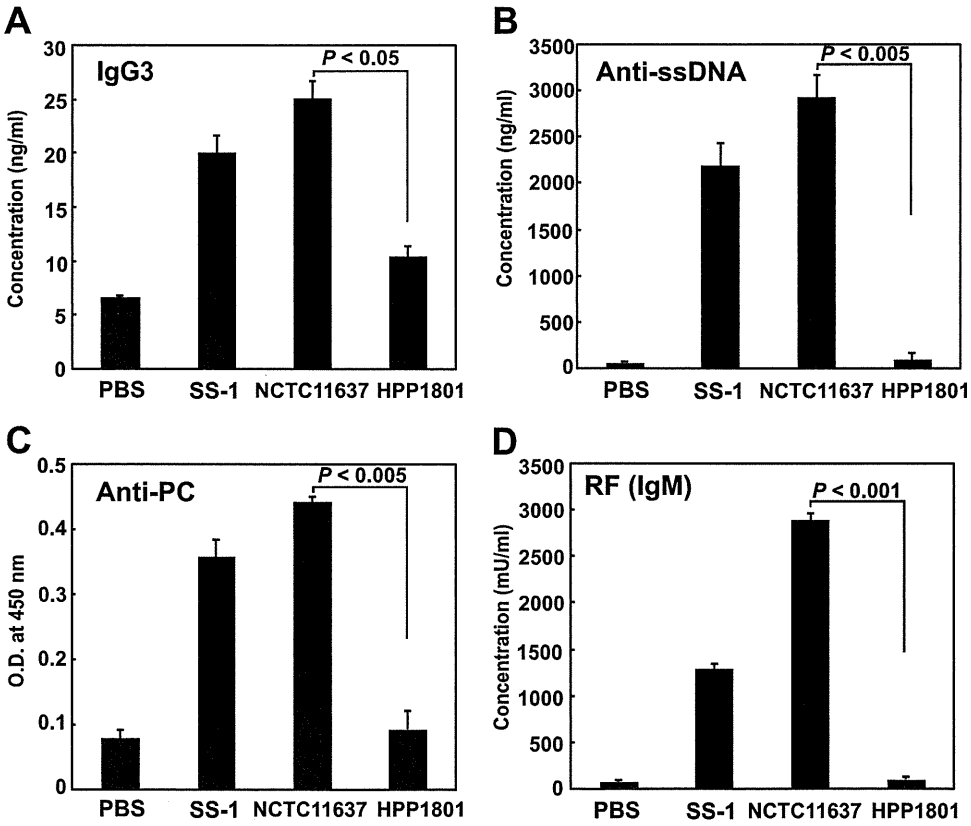

FIG. 4. Secretion of autoantibodies from purified B-1a cells stimulated with fixed plate-coated *H. pylori*. Purified murine B-1a cells (2×10^5) were cultured with either urease-positive *H. pylori* (SS-1 and NCTC 11637) or urease-negative *H. pylori* (HPP1801) fixed by 2% PFA for 10 min and cultured for an additional 7 days, and the supernatants were harvested to measure the production of autoantibodies by ELISA. Results are expressed as means ± SDs ($n = 5$). Statistical significance was determined by the Student *t* test, and the *P* values are given in each graph.

However, we could always obtain far fewer perC B-1a cells than sorted splenic B-1a cells from a mouse. Thus, we used sorted splenic B-1a cells for further experiments.

Detection and localization of *H. pylori* urease. To confirm whether urease is actually secreted from *H. pylori* in the growth state, we examined the bacterial culture supernatant of *H. pylori*. *H. pylori* urease was slightly detected in the culture supernatant of NCTC 11637 isolates with a sensitive ELISA system using highly purified *H. pylori* urease-specific MAb (8, 14) (Fig. 2A). We tried to confirm the results by Western blotting by using whole urease-specific antibody from immune rabbit sera and two *H. pylori* urease-specific MAbs, L2 for the large subunit (UreB) and S2 for the small subunit (UreA), as described in Materials and Methods. As shown in Fig. 2B, similar to the purified *H. pylori* urease, we could detect both the large subunit (UreB) and the small subunit (UreA) in the culture supernatants of both SS-1 and NCTC 11637 by Western blotting. Here, we have also confirmed that HPP1801, a urease-negative isogenic mutant from NCTC 11637, did not express urease (Fig. 2B). These findings indicate that, although the amount was very small, we could detect complete *H. pylori* urease composed of both the large (UreB) and small (UreA) subunits in the culture supernatants of both SS-1 and NCTC 11637.

Then, we examined whether *H. pylori* urease is expressed on/in the bacteria by immunohistochemical staining using anti-*H. pylori* urease-specific antibody. Here, we took advantage of a urease-negative *H. pylori* isolate (HPP1801) as a negative control. We found the expression of *H. pylori* urease on the surface of bacteria rather than inside by both light microscopy (Fig. 3A) and electron microscopy (Fig. 3B). Similar to the previous observation (24), these findings indicate that *H. pylori* expresses urease on its surface and secretes only small amounts of urease. In general, endotoxins, such as LPSs and peptide-glycans (PGs), are components expressed on various pathogens, while exotoxins, such as enterotoxins and verotoxin, are released from the pathogens. The former endotoxins may stimulate immunocompetent cells through TLRs. Thus, we thought that *H. pylori* urease on the bacteria would stimulate innate cells through TLRs.

Stimulation of murine B-1a cells by *H. pylori* urease expressed on the bacterial surface. We then asked whether the *H. pylori* urease expressed on the surface of the bacterium would directly stimulate murine B-1a cells. To keep the expression of urease on the surface, *H. pylori* was fixed with 2% PFA, as indicated in Materials and Methods. We coated a 96-well round-bottom culture plate with the fixed *H. pylori* cells and added purified murine B-1a cells to examine the amount of autoantibodies secreted in the culture supernatant. To eliminate the possibility that B-1a cells were stimulated by components of *H. pylori* other than urease, such as LPS, we cultured B-1a cells with PFA-fixed urease-negative *H. pylori* (strain HPP1801). Consequently, the secretion of various autoantibodies (Fig. 4A to D), such as IgG3 (A), anti-ssDNA (B), anti-PC (C), and RF (D), was detected when B-1a cells were cocultured with the urease-positive *H. pylori* isolate but not with the urease-negative *H. pylori* isolate. It should be noted that the isotypes of the anti-ssDNA and anti-PC autoantibodies secreted by B-1a cells were IgA or IgM (data not shown). These findings strongly suggest that murine B-1a cells can be

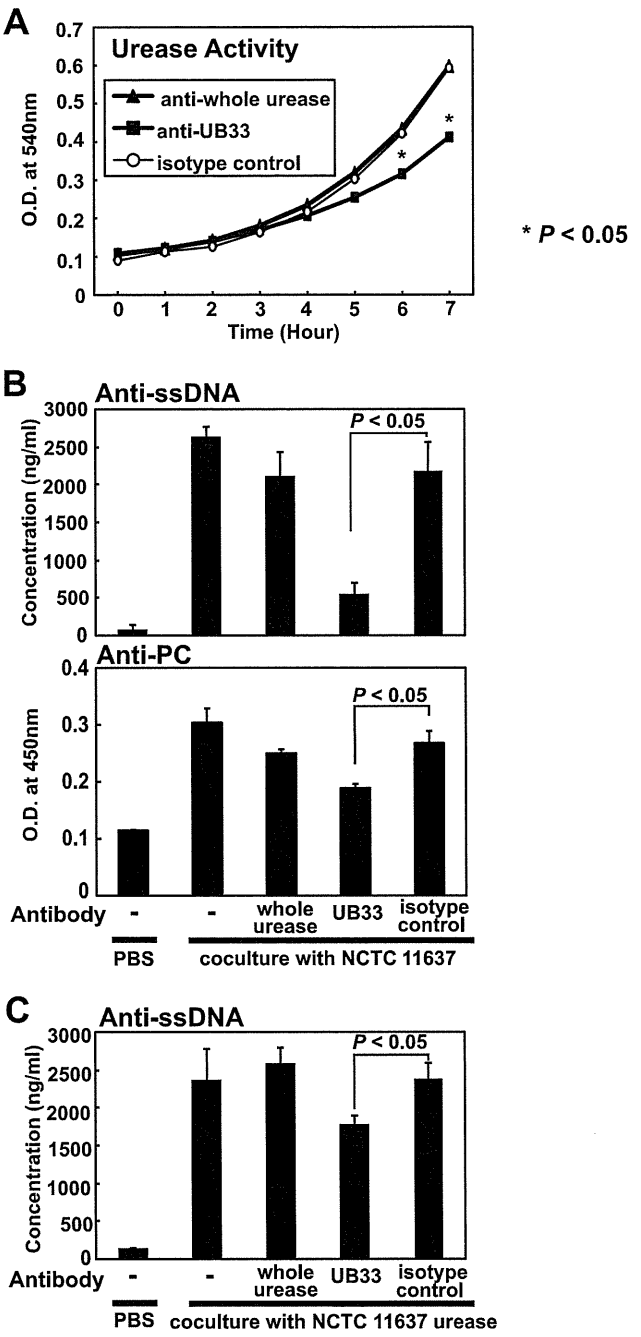

FIG. 5. Effect of *H. pylori*-urease specific antibodies on the secretion of autoantibodies by purified B-1a cells stimulated with *H. pylori* urease. We have identified an epitope for neutralizing antibody, termed the UB-33 peptide, within the large subunit (UreB) of *H. pylori* urease (14). (A) Anti-UB-33-specific rabbit antibody significantly inhibited the enzymatic activity (urea catalysis) of purified urease from the NCTC 11637 isolate (*, $P < 0.005$), although anti-whole urease-specific antibody did not neutralize the activity, similar to the isotype-matched control antibody. Results are expressed as means ± SDs ($n = 5$). (B) Anti-UB-33-specific rabbit antibody significantly suppressed autoantibody secretion by B-1a cells stimulated with urease on the surface of *H. pylori* for 90 min at 37°C. Results are expressed as means ± SDs ($n = 5$). (C) Anti-UB-33-specific rabbit antibody also significantly suppressed autoantibody secretion by B-1a cells stimulated with purified *H. pylori* urease for 90 min at 37°C. Results are expressed as means ± SDs ($n = 5$). Statistical significance was determined by the Student *t* test, and the values are given in each graph.

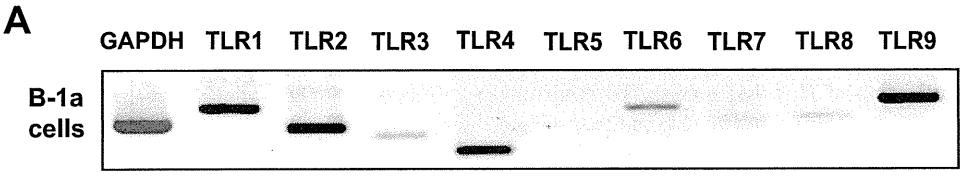

PCR Primers

	forward	reverse
GAPDH	5'-GCCTCAAGATCATCAGCAATGC-3'	5'-ATGCCAGTGAGCTTCCCGTTC-3'
TLR1	5'-GAGCAGAGGCAATTGTGGAC-3'	5'-TGGAGTCTGTTGTAGGACATTATCA-3'
TLR2	5'-CATCACCGGTCAGAAAACAA-3'	5'-GTCACCATGGCCAATGTAGG-3'
TLR3	5'-AGCAACCCTTTCAAAAACCA-3'	5'-CCAATTGTCTGGAAACACCC-3'
TLR4	5'-TCAGAACTTCAGTGGCTGGA-3'	5'-GAGGCCAATTTTGTCTCCAC-3'
TLR5	5'-ACGCCTCATCTAACTGCATA-3'	5'-AAAAGGCTATCCTGCCGTCT-3'
TLR6	5'-CCTGACGAAGCTGACTTTCC-3'	5'-CTATGTGCTGGAGGGTCACA-3'
TLR7	5'-CCACCAGACCTCTTTGATTCC-3'	5'-CCCTCAGGGATTTCTGTCAA-3'
TLR8	5'-CAA ACGTTTTACCTTCTTTGTC-3'	5'-TGAGGTTTTGCAGCAGTTTTGA-3'
TLR9	5'-CCTCCTCCAGAAACTCGATG-3'	5'-AAGAGTGAAAGGCCAAAGCA-3'

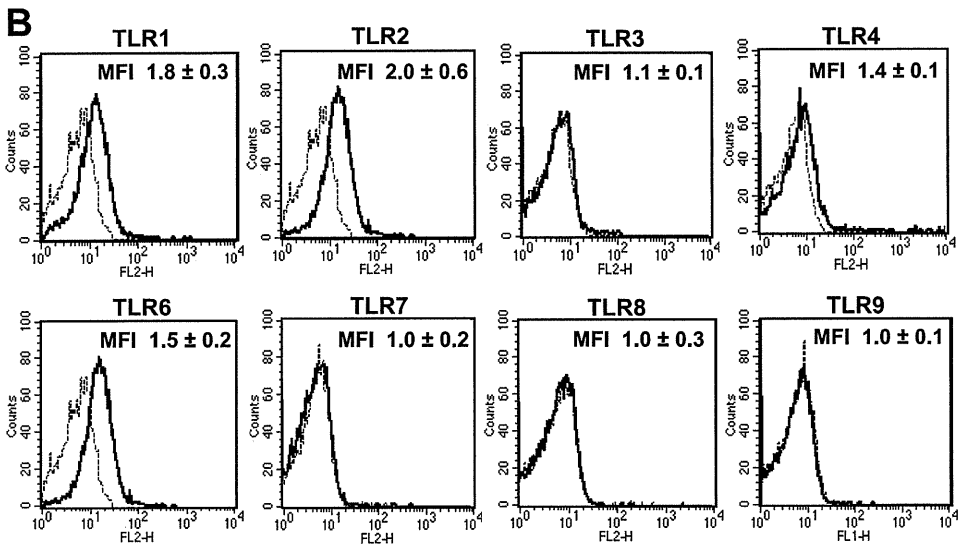

FIG. 6. TLR expression on murine B-1 cells. (A) TLR expression in B-1a cells was analyzed by reverse transcription-PCR. B-1a cells strongly expressed TLR1, TLR2, TLR4, TLR6, and TLR9 and weakly expressed TLR3, TLR7, and TLR8. (B) Surface expression of TLRs on purified B-1a cells was also analyzed by flow cytometry. B-1a cells expressed TLR1, TLR2, TLR4, and TLR6 on their surface. MFI, maximum fluorescence intensity.

stimulated to secrete autoantibodies by *H. pylori* urease expressed on the bacterial surface.

Effect of anti-*H. pylori* urease-specific antibodies on autoantibody secretion by B-1a cells stimulated with bacterium-coated plates. Next, we examined the effects of various *H. pylori* urease-specific antibodies on autoantibody secretion by B-1a cells. As we have reported previously (14), there are two distinct types of *H. pylori* urease-specific antibodies: one can neutralize urease enzymatic activity, and the other cannot, despite its binding capacity. We have identified an epitope for neutralizing antibody, termed the UB-33 peptide, within the large subunit (UreB) of *H. pylori* urease and demonstrated that rabbit immune sera specific for that epitope neutralized urease enzymatic activity (14), although sera from rabbits immunized with purified whole *H. pylori* urease did not.

When strain NCTC 11637 was treated with anti-UB-33-specific antibody, the enzymatic activity of its urease was apparently inhibited, although anti-whole urease-specific antibody did not cause urease inhibition, as seen with the isotype-matched control antibody (Fig. 5A). Also, B-1a cells were less stimulated to secrete autoantibodies with PFA-fixed urease-positive *H. pylori* when the fixed bacteria were pretreated with an excess of purified UB-33-specific rabbit serum than with purified whole *H. pylori* urease-specific serum (Fig. 5B). Similarly, B-1a cells were also less stimulated to secrete autoantibodies with purified *H. pylori* urease pretreated with purified UB-33-specific rabbit serum (Fig. 5C). Moreover, autoantibody production by B-1a cells declined significantly when the enzymatic activity of purified *H. pylori* urease was reduced by heat treatment (data not shown). These findings suggest that

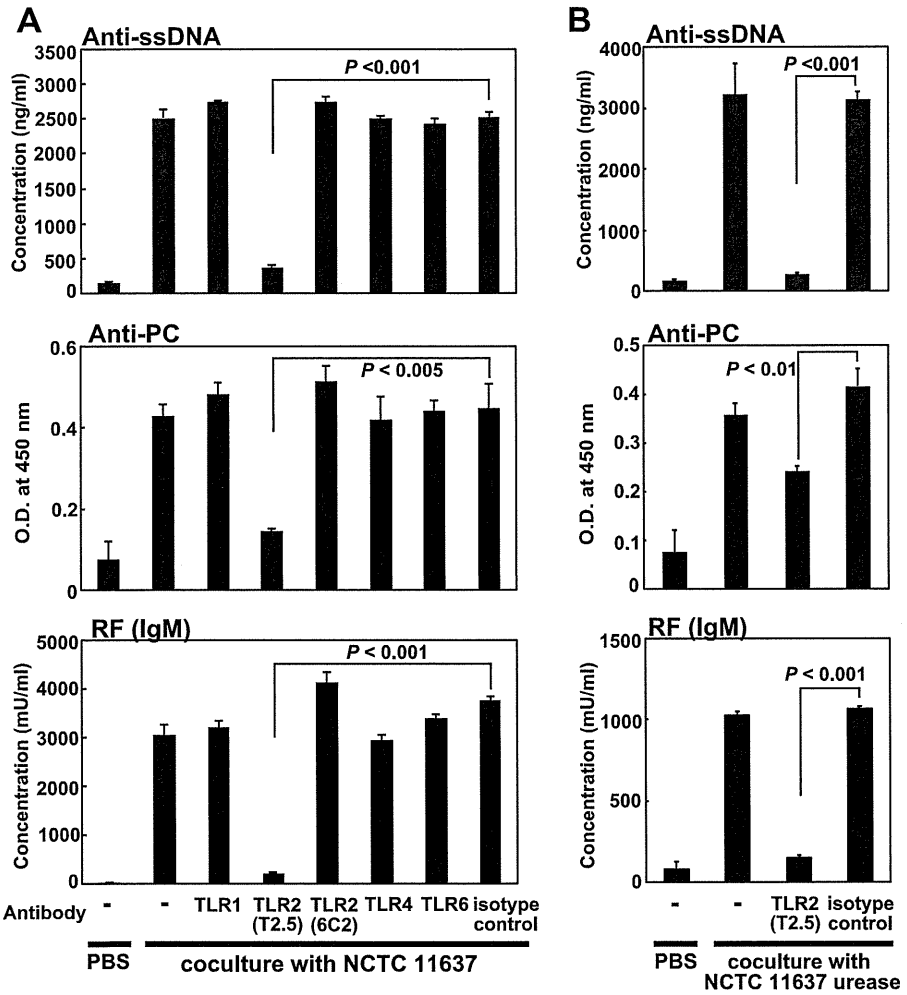

FIG. 7. *H. pylori* urease was a ligand for TLR2 on murine B-1a cells. (A) Purified murine B-1a cells (2×10^5) were incubated for 30 min with either anti-mouse TLR antibodies or an isotype-matched antibody (final concentration, 1 μg/10^6 cells) and washed with culture medium to remove free antibody. Cells were further cultured with *H. pylori* (SS-1 and NCTC 11637)-precoated round-bottom 96-well plates for an additional 7 days, and autoantibody secretion in the supernatant was measured. Pretreatment with anti-mouse TLR2 antibody (T2.5) significantly inhibited the secretion of autoantibodies. Results are expressed as means ± SDs ($n = 7$). (B) Purified murine B-1a cells (2×10^5) were incubated for 30 min with either anti-mouse TLR2 antibody (T2.5) or an isotype-matched antibody and further cultured with 10 μg/ml purified *H. pylori* urease for 7 days. Pretreatment with the anti-mouse TLR2 antibody (T2.5) again significantly inhibited the secretion of autoantibodies. Results are expressed as means ± SDs ($n = 7$). Statistical significance was determined by the Student *t* test, and the values are given in each graph.

murine B-1a cells were more strongly activated to secrete autoantibodies by *H. pylori* urease expressed on the bacterial surface that retained enzymatic activity.

***H. pylori* urease was a ligand for TLR2 on murine B-1a cells.** These results indicate that the *H. pylori* urease retaining enzymatic activity appears to potently stimulate murine B-1a cells to produce various autoantibodies. The fact that B-1a cells were directly activated by urease on the bacterial surface, like endotoxins such as LPSs and PGs, within a few hours suggests that some innate TLRs on B-1a cells may interact with *H. pylori* urease as an active bacterial functional component. Thus, we analyzed the expression of TLRs on $CD5^+$ B-1a cells and found that the B-1a cells expressed TLR1, TLR2, TLR4, and TLR6 on their surface (Fig. 6A and B). Then, we examined which TLRs might interact with *H. pylori* urease by blocking each TLR on B-1a cells with each specific antibody. Although TLR1-, TLR4-, and TLR6-specific MAbs did not affect the secretion of autoantibodies by B-1a cells stimulated with *H. pylori* urease, secretion was significantly inhibited when TLR2-specific MAb (T2.5) (19) was added to the culture (Fig. 7A). Moreover, to prove that *H. pylori* urease was an actual ligand for TLR2, murine B-1a cells pretreated with anti-TLR2 MAb were stimulated with purified *H. pylori* urease. Although B-1a cells pretreated with anti-TLR2 MAb (T2.5) did not secrete autoantibodies (Fig. 7B), pretreatment with another TLR2-specific MAb, 6C2 (23), whose binding site was different from that of T2.5, did not inhibit the secretion of autoantibodies. Furthermore, B-1a cells obtained from TLR2-knockout ($TLR2^{-/-}$) BALB/c mice were not stimulated to secrete autoantibodies by bacterium (strain SS-1 or NCTC 11637)-coated plates (Fig. 8A) or the purified *H. pylori* urease of strain SS-1 or NCTC 11637 (Fig. 8B).

These findings collectively suggest that some portion of innate TLR2 on B-1a cells may interact with functional bacterial

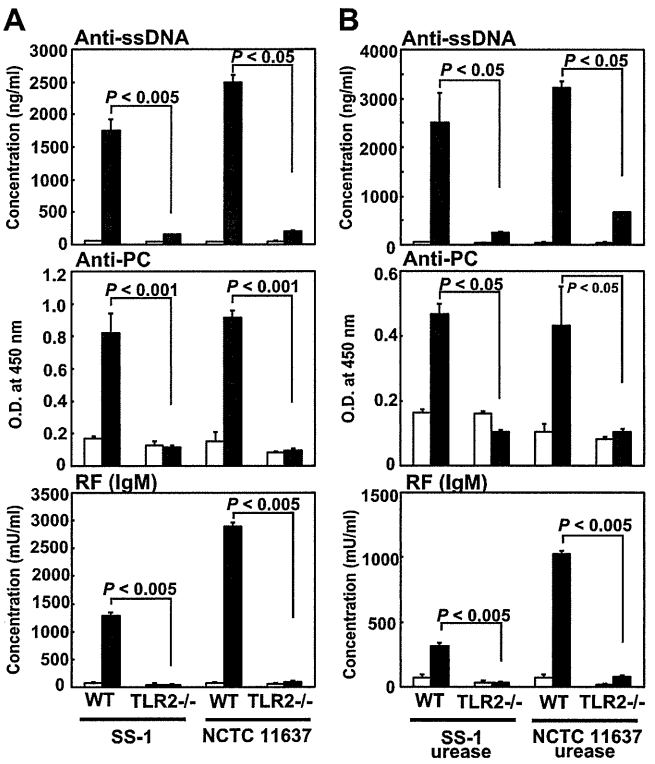

FIG. 8. Murine B-1a cells from TLR2-knockout ($TLR2^{-/-}$) BALB/c mice did not respond to either *H. pylori* (SS-1 or NCTC 11637)-coated plates (A) or purified *H. pylori* (SS-1 or NCTC 11637) urease (B). (A) Two × 10^5 purified murine B-1a cells from either normal wild-type BALB/c mice (WT) or $TLR2^{-/-}$ mice were cultured in plates precoated with *H. pylori* (SS-1 or NCTC 11637) (filled columns) or PBS (open columns) for 7 days, and autoantibody secretion in the culture supernatant was measured. Results are expressed as means ± SDs (n = 5). (B) Purified murine B-1a cells (2 × 10^5) from either normal wild-type BALB/c mice or $TLR2^{-/-}$ BALB/c mice were cultured with 10 μg/ml purified *H. pylori* urease (filled columns) or PBS (open columns) for 7 days, and autoantibody secretion in the culture supernatant was measured. Results are expressed as means ± SDs (n = 5). Statistical significance was determined by the Student t test, and the values are given in each graph.

urease expressed on the surface of *H. pylori* to secrete various autoantibodies.

Detection and localization of *H. pylori* LPS. There are some reports showing that *H. pylori* LPS can stimulate TLR2 rather than classical TLR4 for LPS in other bacteria. Indeed, Smith et al. recently reported (27) that *H. pylori* LPS detected by anti-Lewis x (Le^x) (clone P12) or anti-Lewis y (Le^y) (clone F3) murine IgM MAbs (21) stimulated cells to induce a set of chemokines in a TLR2-dependent fashion. Thus, to eliminate the possibility that the *H. pylori* LPS stimulates B-1a cells to secrete autoantibodies, we tried to identify the Le^x and/or Le^y antigen on the urease-negative HPP1801 mutant that did not stimulate B-1a cells. As demonstrated in Fig. 9, although the expression of Le^x antigen was very weak, apparent Le^y antigen expression was seen on the surface of the HPP1801 mutant as well as isolates NCTC 11637 and SS-1 by light microscopy (Fig. 9A). Also, we could detect Le^y antigens in the purified LPSs obtained from HPP1801 as well as NCTC 11637 and SS-1 by Western blotting (Fig. 9B). These results clearly indicate that *H. pylori* LPS will not stimulate B-1a cells to secrete autoantibodies via TLR2.

DISCUSSION

There are two distinct types of murine B cells, B-1 and B-2 cells. Although B-2 cells are conventional T-cell-dependent B cells, in that T cells help B cells to promote their clonal expansion, somatic hypermutation, isotype switch, and differentiation into antibody-secreting cells, B-1 cells, particularly B-1a cells expressing CD5, showing an enriched expression of autoreactive B-cell-antigen receptors, produce several types of natural autoantibodies (11).

In the present study, we found that murine B-1a cells can be stimulated to produce various autoantibodies, such as anti-ssDNA, anti-PC, and RF, by *H. pylori* urease expressed on the surface of the bacteria. This unique response seems to be mediated through the direct interaction between TLR2 on B-1a cells and urease on the bacteria, indicating that *H. pylori* urease acts like a bacterial endotoxin, such as PG or LPS, rather than an exotoxin released from the bacteria. Indeed, we have shown here that *H. pylori* urease was expressed on the bacterial surface and proved that *H. pylori* (either NCTC 11637 or SS-1 isolate)-coated plates bearing bacterial urease on the surface stimulated B-1a cells to produce autoantibodies, although plates coated with urease-negative *H. pylori* HPP1801, which originated from NCTC 11637, did not. These findings indicate that bacterial urease expressed on *H. pylori* but not other products, like LPS or secreted *H. pylori*-associated toxins, such as cytotoxin-associated gene A (CagA) or vacuolating cytotoxin (VacA), is a ligand for TLR2 recognition by B-1a cells.

Moreover, it should be noted that the enzymatic activity of urease on PFA-coated bacteria was maintained and the magnitude of production of autoantibodies by B-1a cells was markedly inhibited when the enzymatic activity of *H. pylori* urease was blocked with UB-33-specific neutralizing antibody (14) but not with urease-specific antibody without a neutralizing capacity. Although this is caused by the steric hindrance of binding due to the attached anti-urease-specific antibody, the results reveal that the innate TLR2 on B-1a cells may have a potency to distinguish the functional enzymatic capacity of bacterial ligands, and thus, those B-1a cells can recognize whether the pathogens that have intruded the body express live functional products. We are currently planning to immunize BALB/c mice with the UB-33 peptide plus an appropriate adjuvant to see whether neutralizing antibodies against *H. pylori* urease can be obtained and the production of various autoantibodies can be manipulated in the presence of *H. pylori* or its urease *in vivo*.

To our knowledge, only a few reports have demonstrated that innate TLRs can discriminate between functional and damaged ligands on pathogens; for example, intestinal acyloxyacyl hydrolase, which cleaves acyl chains from the lipid A portion of LPS, downmodulates the proinflammatory response through TLR4-mediated innate immune signaling (6), and in mice lacking this enzyme, acylated LPS persists for longer periods after infection with Gram-negative bacteria and elicits increased B-cell proliferation as well as antibody production (18). In addition, alkaline phosphatase in the brush border of